Metagenomics of the Built Cultural Heritage: Microbiota Characterization of the Building Materials of the Holy Aedicule of the Holy Sepulchre in Jerusalem

Ekaterini T. Delegou [1], Christos Karapiperis [2,3,4], Zoe Hilioti [4,5], Anastasia Chasapi [3,4] Dimitris Valasiadis [4], Athanasia Alexandridou [4], Vasiliki Rihani [4], Maria Kroustalaki[3,4], Theodore Bris[1], C. A. Ouzounis [2,3,4], Antonis Salakidis [4], and Antonia Moropoulou [1,*]

[1] Laboratory of Materials Science & Engineering, School of Chemical Engineering, National Technical Uni-versity of Athens (NTUA), 9 Iroon Polytechniou Str., Zografou Campus, Athens, 15780, Greece
[2] School of Informatics, Aristotle University of Thessaloniki, Thessalonica, 54124, Greece
[3] Chemical Process & Energy Resources Institute, Centre for Research & Technology Hellas, Thermi, Thessalonica, 57001, Greece
[4] DNASequence SRL Hellas, Thermi, Thessalonica, 57001, Greece
[5] Institute of Applied Biosciences, Centre for Research & Technology Hellas, Thermi, Thessalonica, 57001, Greece

Received: 19/01/2022
Accepted: 02/02/2022
Corresponding author: Antonia Moropoulou (amoropul@central.ntua.gr)

1. ABSTRACT

In this study, the presence of microbial communities in the building materials of the Holy Aedicule via amplicon metagenomics is established. Ten samples in total are examined consisting of five mortar samples, two marble samples and three Holy Rock samples. They all are of high importance from a historical perspective, and they are collected from various locations of the Holy Tomb Chamber. This is the first time that samples from the Holy Aedicule have been analysed by metagenomics, and the documented microbial communities can serve as a benchmark of the monument's state at the time of sampling and can therefore be used in any future works in regard to the sustainability of the monument. It is observed that all the examined samples are colonized by certain common and more importantly distinctive microbial communities, from several genera. Particularly, the species *Pseudomonas aeruginosa, Acinetobacter johnsonii, Chroococcidiopsis thermalis PCC 7203, Loriellopsis cavernicola, Zhihengliuella somnathii, Massilia atriviolacea* and *Massilia aurea* display the highest relative abundances in all the examined samples, compared to the rest of the identified species. Furthermore, a machine learning method is implemented to rank, at the genus level, the most characteristic low abundance microbiota communities among the examined samples, while a cluster analysis, based on the kind and the abundance of all the species identified in each sample, is also performed. The above mentioned bioinformatics approaches offer additional insights featuring samples interrelation, and they are interpreted using building materials data, archaeometry data, as well as historical evidence, presented in previous works. Thus, a new potential about the microbiota characterization in built cultural heritage is highlighted and suggested.

KEYWORDS: building materials, stone, mortar, marble, metagenomics, bioinformatics, machine learning, Holy Sepulchre

1. INTRODUCTION

Metagenomics is the application of modern genomics techniques to study communities of microbial organisms directly in their natural environments, bypassing the need for isolation and lab cultivation of individual species (Ramazzotti & Bacci, 2018). During the last decade, modern sequencing tools, such as metagenomics, dominate to classical microbiology methods thanks to the formers' accuracy in isolating the bacterial strains and the huge dataset of molecules that is detected (Vilanova & Porcar, 2020). As a consequence, metagenomics and bioinformatics application speed up the procedures of characterization of microbial communities inhabiting the investigation samples. On the contrary, traditional microbial detection methods are characterized by isolation, which means that only a small percentage of microorganisms developed on the examined object can be detected through this approach. Therefore, the –omics technologies have already been largely used in several scientific fields, such as biology (Wei et al., 2019), biotechnology (Schmeisser et al., 2007), medicine (Schommer & Gallo, 2013), agriculture (Meunier & Bayır, 2021) etc. Evidently, this has been possible thanks not only to the technological advances of Next Generation Sequencing techniques and hardware, but also to the development of efficient bioinformatics workflows for the analysis of produced complex data such as in the case of metagenomics experiments (Kunin et al., 2008; Luz Calle, 2019).

Next generation sequencing takes an advantage role in cultural heritage and building environment in the last few years, as well (Adamiak et al., 2018; Dyda et al., 2019; Nir et al., 2021). In fact, various monuments have been constructed by natural stones, which besides their abiotic origin; they are highly affected by bio deterioration (Schröer et al., 2021). Therefore, the identification of the microbial communities, as well as the implementing of the suitable microbiological media, have been special issues for the scientists as much as the norm interest in human aDNA (Evison, 2014; Liritzis et al., 2021). These prospections become more significant, considering the favorable role, which microorganisms can play on several building materials and especially on natural stones, through bio mineralization (Jroundi et al., 2017). As a consequence, new sequencing methodologies have led to the development of alternative consolidation methods that is bio consolidation, avoiding the conventional intervention techniques (Delgado Rodrigues & Ferreira Pinto, 2019). Finally, apart from the above mentioned advantages of next generation sequencing, they can also provide chronological determination of significant events happened in the past, such as identification of the source, interventions history and storage conditions (Teasdale et al., 2017). In particular, microorganisms leave traces on and in the examined objects, which are represented by DNA; the similarity of which probably indicates the same history of the investigating objects (Piñar et al., 2019).

The Holy Aedicule is considered one of the holiest places among Christians, since the Tomb of Christ is believed to be laid within the structure. In the cave tomb of Jesus Christ, in 136 AD, the Roman Emperor Hadrian constructed a Capitolium, since Jerusalem was named Aelia Capitolina and was rebuilt as a typical Roman city. About 200 years later, in 325/326 AD, during the era of Constantine the Great, Saint Helena discovered the Tomb of Christ, and she formulated the burial chamber in a polygonal ciborium-type structure (Aedicule) (Cameron & Hall, 1981; Patrich, 2002). In 614 AD, when the Persians conquered Jerusalem, the Church of Resurrection was significantly destroyed (Meško, 2016), and thus in 626 AD, Modestos, the Patriarch of Jerusalem, restored the Church of Resurrection within the next four years. In 1009 AD the Fatimid Caliph, al-Hākim bi-Amr Allāh, took control of Jerusalem and the Church of Resurrection was among the many Pilgrimage Sites that he destroyed (Mitropoulos, 2009). However, shortly after ~1012-1023 AD, Maria the Christian mother of Al Hakim, is considered to have rebuilt the Resurrection Church (Patrich, 2002). During the first half of the 11th century (~1037-1040 AD) the Byzantine Emperor Michael IV the Paphlagonian (1034–41 CE), or the Emperor Constantine IX Monomachos (1042–1048 CE), or both, reconstructed the Holy Site which was damaged by a major earthquake in 1034 (Patrich, 2002). Shortly after, in 1099 to 1187 AD, the Crusaders added one more room to the Aedicule, named ever since "the Chapel of the Angel", expanding it to the east (Mitropoulos, 2009; Patrich, 2002). Yet, in 1244 AD, the Aedicule was defiled and parts of the Holy Tomb Chamber were removed by the Khwarismian horsemen, who had entered Jerusalem (Patrich, 2002). Since the shrine was not restored for about 500 years and in parallel was severely damaged by major earthquakes in 1453 AD, and 1545 AD, the Custos of the Franciscan Order, Fra Bonifacio da Ragusa, conducted an important restoration of the Holy Aedicule in 1555 AD (Mitropoulos, 2009; Patrich, 2002). Another major restoration followed in 1809-1810 AD by the architect Kalfa Komnenos,

after the devastating fire of 1808. During Komnenos restoration the Holy Aedicule took its present form (Mitropoulos, 2009; Patrich, 2002). Furthermore, during the British Mandate in 1947 AD, an external iron frame was placed to strengthen temporally the structure, preventing further masonry deformations (Freeman, 1947; Patrich, 2002).

Finally, in 2015 AD the National Technical University of Athens (NTUA) studied the causes of the structure deformation, designed and suggested rehabilitation strategies, during the project "Integrated Diagnostic Research Project and Strategic Planning for Materials, Interventions Conservation and Rehabilitation of the Holy Aedicule of the Church of the Holy Sepulchre in Jerusalem" (Moropoulou et al., 2016, 2017), after the invitation of His Beatitude, Patriarch of Jerusalem Theophilos III. This study initiated a rehabilitation project at 2016-2017 AD supervised by NTUA, and it was implemented after the historical Common Agreement of the three Christian Communities responsible for the Holy Sepulchre (Alexakis et al., 2018; Apostolopoulou et al., 2018; Georgopoulos et al., 2017; Moropoulou et al., 2018a).

Figure 1. The Holy Aedicule of the Holy Sepulchre as it stands today, viewed from the south.

NTUA studies about the monument have pointed out that the high thermo-hygric loads detected are present due to the large number of pilgrims that continuously visit the monument, as well as due to the intense rising damp from the underground sewage network and infrastructures (Moropoulou et al., 2018a). Thus, the identification of the microbiota of the Holy Aedicule's building materials gets even more important as sustainability issues will need to be further addressed in the future. In this framework, this study presents the advanced technologies of metagenomics and bioinformatics utilized on samples of building materials of the Holy Aedicule, for their microbial characterization, in regards of species type and abundance. Furthermore, the samples under investigation are considered of high importance from a historical/archaeological perspective, and they include Holy Rock, marbles and mortars' samples, collected from various locations of the monument. Subsequently, machine learning and cluster analysis are applied to investigate possible interrelations among the metagenomics results with the results of previous works regarding building materials data, archaeometry data and historical data.

2. MATERIALS AND METHODS

2.1 DESCRIPTION OF THE HOLY AEDICULE SAMPLES

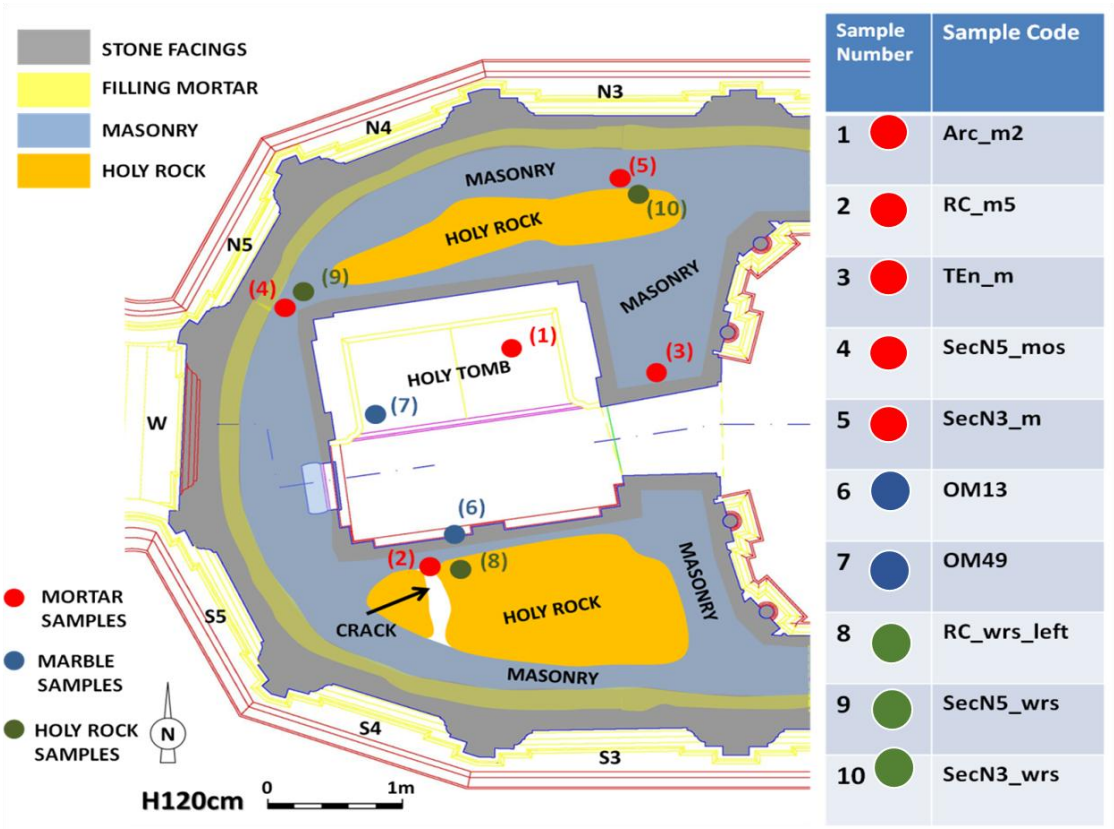

Figure 2. The location and coding of all the investigated samples depicted on the ground plan of the Tomb Chamber (ground plan modified from (Lampropoulos et al., 2017)**).**

The samples under investigation were collected from several locations of the Holy Tomb Chamber of the Holy Aedicule, and their sampling points are depicted in Figure 2. The Holy Aedicule is an indoor, complex and multi-layered structure consisting of (from the exterior to the interior), exterior stone facings, filling mortar, rubble masonry, Holy Rock (found embedded in the masonry only at the north and south parts of the Holy Tomb Chamber), filling mortar and interior marble facings (Figure 2). Ten samples in total are examined consisting of five mortar samples, two marble samples and three Holy Rock samples.

Both the mortar sample Arc_m2 and the marble sample OM49 were located inside the Holy Tomb and were collected when it was opened for once more after about five centuries, during grouting works (Figure 3a, b) (Lampropoulos et al., 2022). When the amber hued marble plate was shifted out of position, a fragmented grey marble plate and the Holy burial bed rock could be observed. The Arc_m2 sample was collected from the bedding mortar layer placed between the fragmented grey marble plate and the Holy burial bed rock (Figure 3d). In the areas where the grey marble plate was absent, filling material was evident, and a marble fragment, consisting sample OM49, was found (Figure 3a, c). The important historical value of the collected samples was further revealed when Optically Stimulated Luminescence (OSL) results estimated that the gypsum based bedding mortar Arc_m2 is of the Constantinean era (Calendar centered Age: middle 4th century CE, 345 ± 230 CE); and therefore it was concluded that the grey fragmented marble plate was also placed during the Constantinean era (Moropoulou et al., 2018b). Furthermore, the petrographic study and the isotopic analysis of $\delta^{18}O$ and $\delta^{13}C$, demonstrated that the marble fragment (sample OM49), and the fragmented lower Constantinean plate are Proconnesos marbles of variety type I (Moropoulou et al., 2019). In addition, besides their common origin, both Constantinean plate and marble fragment are of the same thickness, a fact that presumably shows that OM49 is the decorative edge of the lower grey Constantinean plate (Moropoulou et al., 2019).

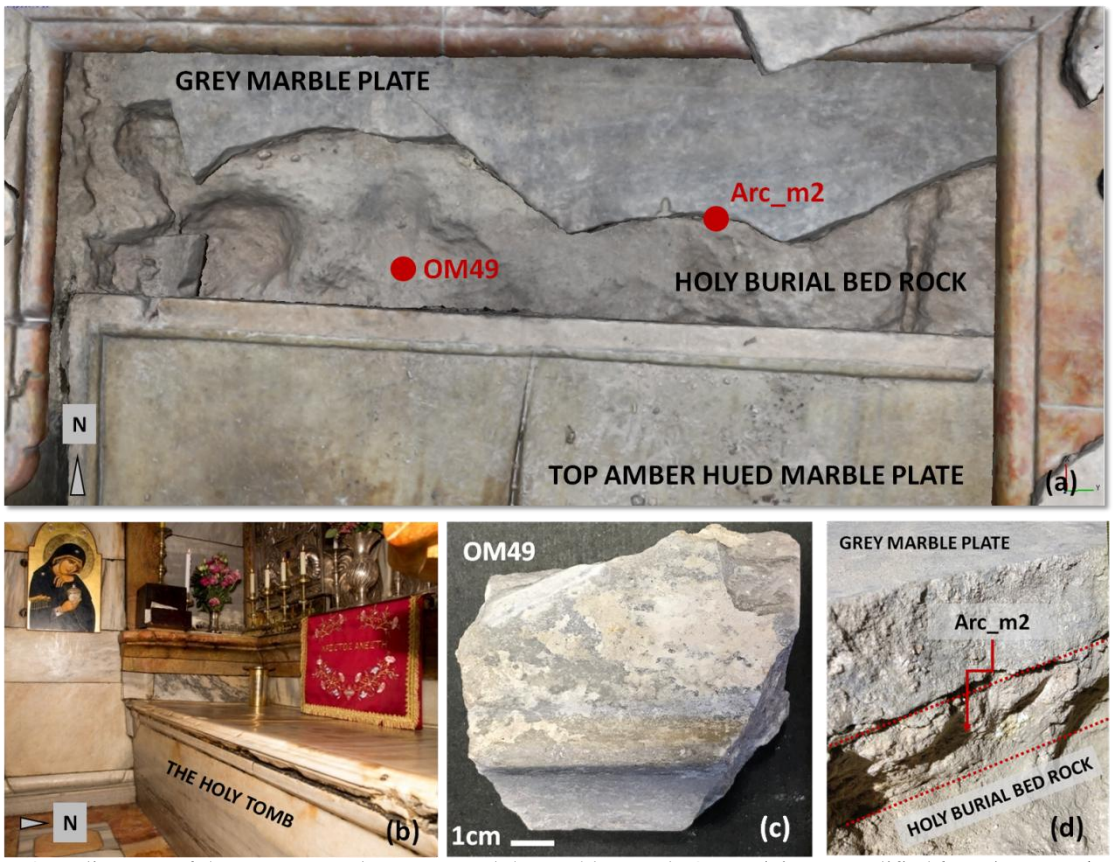

Figure 3. Sampling area of the mortar sample Arc_m2 and the marble sample OM49, (picture modified from (Moropoulou et al., 2018b; Moropoulou et al., 2019)**). (a) View of the top amber hued marble plate out of place, the Holy Burial Bed Rock and the fragmented grey marble plate, along with the sampling point of mortar Arc_m2 and the location where sample OM49 was found, when the Holy Tomb was open; (b) the Holy Tomb viewed from southeast with the top amber hued marble plate in place; (c) OM49 sample, the marble fragment found inside the Holy Tomb; (d) the sampling location of the mortar sample Arc_m2, between the grey marble plate and the Holy burial bed rock.**

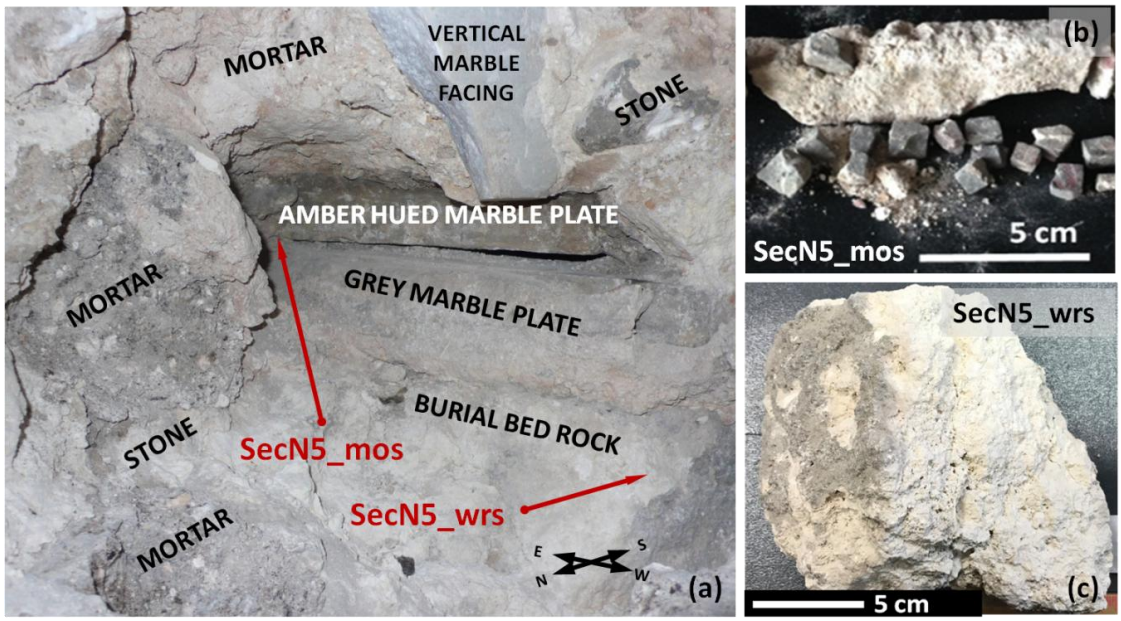

Figure 4. Sampling area of the mortar sample SecN5_mos and the Holy Rock sample SecN5_wrs (picture modified from (Moropoulou et al., 2018b)**); (a) Location of the mortar sample SecN5_mos and the Holy rock sample SecN5_wrs in the section area of panel N5, viewed from northwest; (b) sample SecN5_mos, where loosely attached tesserae are evident; (c) sample SecN5_wrs.**

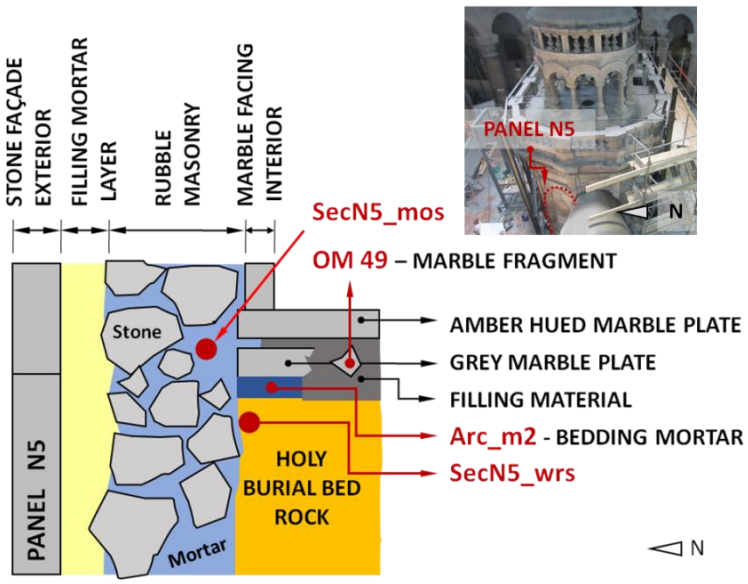

Figure 5. Schematic representation in section of the location and relevant proximity of the samples Arc_m2, OM49, SecN5_mos, and SecN5_wrs (picture modified from (Moropoulou et al., 2018b; Moropoulou et al., 2019)**). Photo in the top right depicts Panel N5 viewed from top northwest, before stone facings removal.**

During the rehabilitation works of 2016-2017, certain parts of the masonry of the Holy Aedicule were revealed by temporary removing the external stone facings. These areas were named Panels, and they were coded according to the facade orientation (N for north, S for south, etc), and numbered 1 to 5 in regard to their proximity to the east façade, where the entrance of the monument is (Figure 2). Masonry sections were opened at some of these panels, depending on the restoration needs, and when a masonry section was opened at the lower part of Panel N5, we managed to observe the Holy Tomb from its northwest corner, noticing clearly the Holy burial bed rock, the grey marble plate and the amber hued marble plate (Figures 4a and 5). Sample SecN5_wrs was collected by the northwest edge of the Holy burial bed rock, while the mortar sample SecN5_mos was found inside the section having on its surface several black crusted tesserae (Figure 4b). SecN5_mos is also gypsum based mortar and it was dated by OSL back to Renaissance era (Calendar centered Age: middle 16th century CE, 1560 ± 70 CE), corresponding to the period of the Restoration by Boniface of Ragusa (Moropoulou et al., 2018b). SecN5_mos is possibly the result of conservation interventions of an older mosaic during the restoration of Boniface of Ragusa, not only because of the disordered positioning of the tesserae in the mortar (Figure 4b), but also because of some historical testimonies corresponding to 1047 and 1149 CE that describe the presence of mosaics in the Holy Aedicule (Patrich, 2002). Therefore, this is not the original location of sample SecN5_mos, and it seems that it was placed in the masonry during restorations that followed the Boniface of Ragusa era (most probably during the Komnenos restoration), in the concept of preserving older Aedicule parts through setting them in newer phases (Moropoulou et al., 2018b).

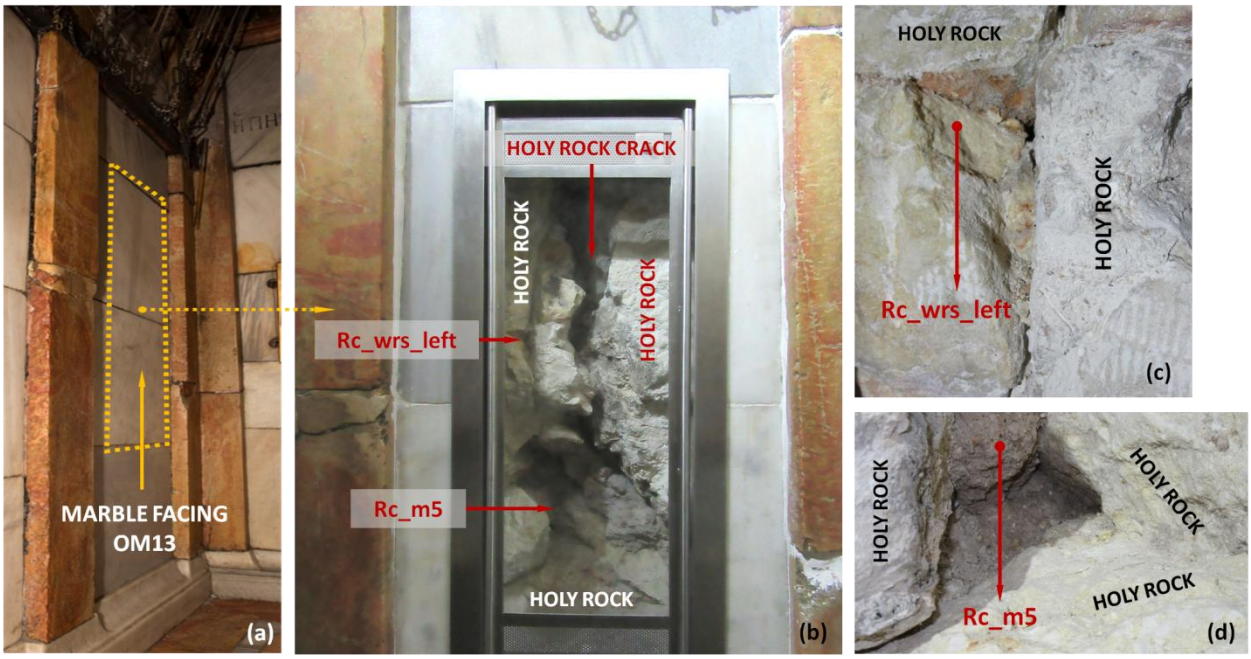

Figure 6. Sampling area of the marble sample OM13, mortar sample RC_m5 and the Holy Rock sample RC_wrs_left (picture modified from (Moropoulou et al., 2018b)**); (a) the area where the marble facing is still in place, before the installation of the observation window of the Holy Rock, showing the sampling location of sample OM13; (b) Location of the Holy rock sample RC_wrs_left and the mortar sample of RC_m5, in the window area that was installed to provide visibility of the Holy rock, opposite of the Holy Tomb; (c) the exact sampling point of RC_wrs_left; (d) the exact sampling point of sample RC_m5.**

During grouting works, two marble slabs at the interior side of the south wall of the Holy Aedicule, opposite to the Holy Tomb, were removed to monitor the intervention (Lampropoulos et al., 2022). The marble sample OM13 was collected from the lower of these two slabs (Figure 6a), while after the completion of the grouting, the three Christian Communities decided to permanently install an observation window of the Holy Rock (Figure 6b). Sample RC_wrs_left was collected from the Holy Rock part left to the vertical crack, and the sample RC_m5 was collected from the mortar filling the lower part of the vertical crack of the Holy Rock (Figures 6c, d). OSL dating of the gypsum based mortar RC_m5 revealed a Calendar centered Age at late 16th century CE, in 1570 ± 68 CE, that is the era of the Restoration of 1555 by Boniface of Ragusa (Moropoulou et al., 2018b). This mortar sample was taken within the Holy Rock crack, indicating that some marble panels of the Holy Aedicule interior were placed or replaced or even reattached during the Boniface restoration. Petrography study and isotopic analysis of $\delta^{18}O$ and $\delta^{13}C$ values demonstrated that OM13 is a Proconnesos marble of variety type I and it could have originated only from the ancient quarry C5b of the Proconnesos island (Moropoulou et al., 2019). This marble slab could have been placed into its current position by Boniface of Ragusa during the restoration interventions of the Holy Rock crack. Yet, there is a possibility that this facing was first placed during the Constantinean era and reattached by Boniface of Ragusa, since a mortar sample (not examined in this study), which was located behind a marble slab placed above the one investigated here, was dated by OSL to 335 ± 235 CE, that is the Constantinean era (Moropoulou et al., 2018b; Moropoulou et al., 2019).

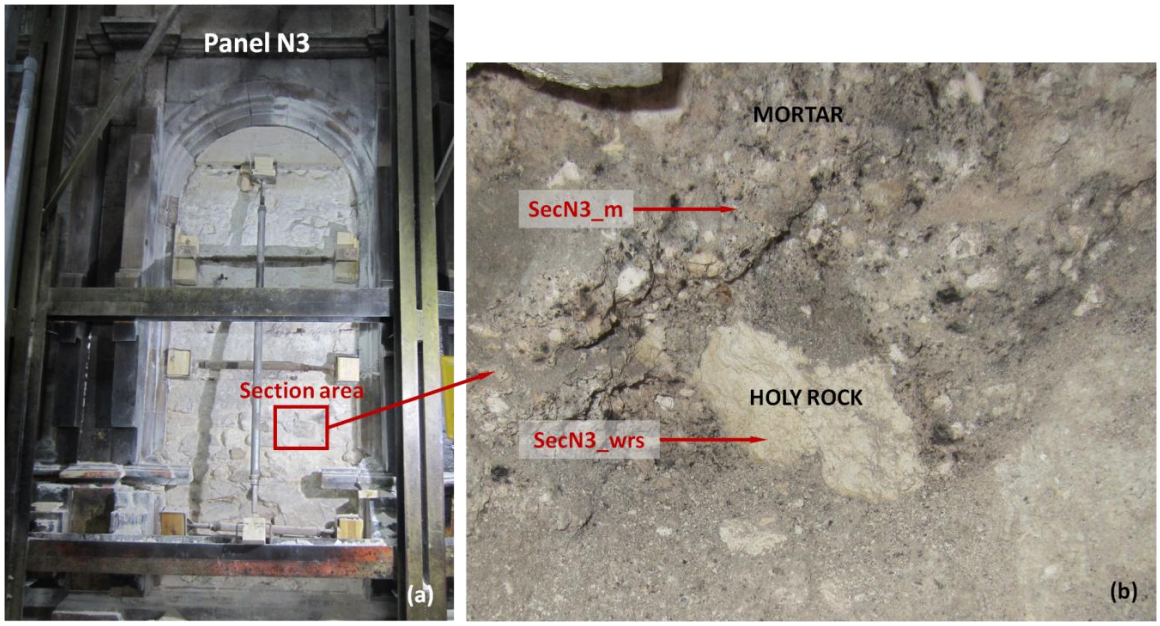

Figure 7. Sampling area of the mortar sample SecN3_m and the Holy Rock sample SecN3_wrs (picture modified from (Moropoulou et al., 2018b)**); (a) Photo of the panel N3, after the stone facings removal, showing the location of the section area; (b) location of mortar sample SecN3_m, and the Holy rock sample SecN3_wrs in the section area of panel N3.**

Respectively to the procedure described about Panel N5, during the inner masonry restoration of Panel N3, a masonry section was opened (Figure 7a). Several types of stones, mortars and the Holy rock could be observed in Panel N3 section, and thus the sample SecN3_wrs was collected from the Holy rock, while the sample SecN3_m was collected from the mortar surrounding the Holy Rock (Figure 7b). OSL results about the lime based mortar SecN3_m resulted in a Calendar centered Age of early 19th century CE, in 1815 ± 32 CE, attributing this sample to the Reconstruction of Kalfas Komnenos (Moropoulou et al., 2018b); verifying the historic evidence that Komnenos had fully restored the masonry behind the exterior stone facings.

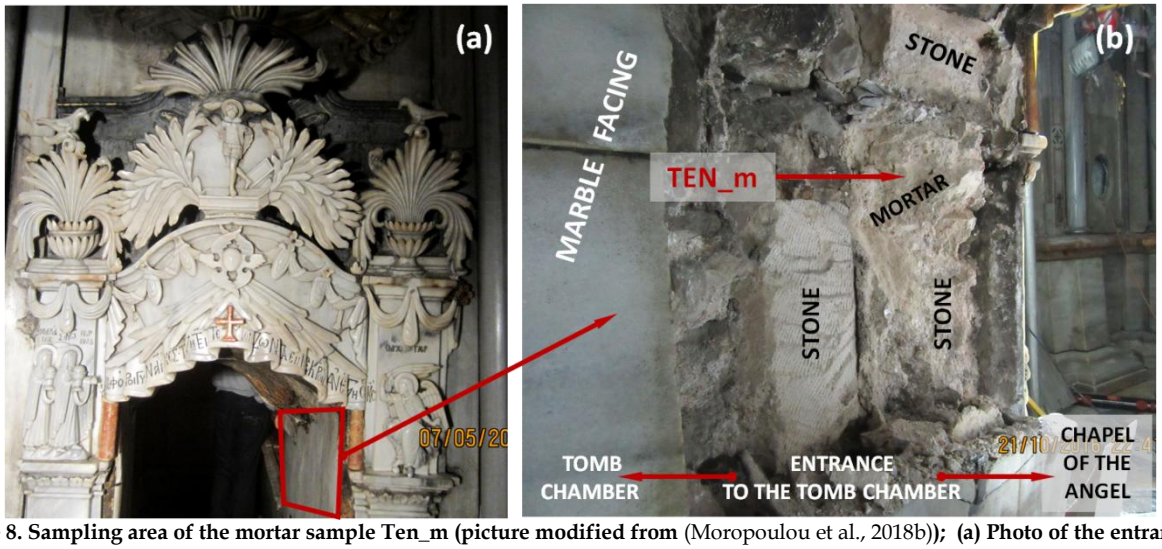

Figure 8. Sampling area of the mortar sample Ten_m (picture modified from (Moropoulou et al., 2018b)**); (a) Photo of the entrance of the Holy Tomb Chamber viewed by the east, showing the marble facing in place; (b) location of sample Ten_m when the marble facing was temporally removed.**

The temporary removal of the interior marble facing at the low entrance of the Holy Tomb Chamber, permitted the inspection and restoration of this masonry part, where the mortar sample Ten_m was collected (Figure 8). OSL study resulted in a Calendar centered Age of middle 11th century CE, in 1040 ± 150 CE, dating this gypsum based mortar to the Byzantine reconstruction of the Aedicule, which it is ascribed to Byzantine Emperors Michael the Paphlagonian (1034–41 CE), and/or Constantine Monomachos (1042–1048

CE), (Moropoulou et al., 2018b). However, due to measurement uncertainty, it cannot be excluded that this area could have been restored by the Crusaders (1099 CE) (Moropoulou et al., 2018b).

The following table summarizes the type and composition of the investigated samples, as well as the results of the OSL dating for the mortar samples based on the results demonstrated in previous works (Moropoulou et al., 2018b; Moropoulou et al., 2019), and shortly described above.

Table I. Type and composition of the investigated samples, and OSL dating results for the mortar samples (Moropoulou et al., 2018b; Moropoulou et al., 2019),

Sample Code	Type and composition	OSL dating
Arc_m2	Gypsum based mortar	345 ± 230 CE, Constantinean era
RC_m5	Gypsum based mortar	1570 ± 68 CE, Boniface of Ragusa Restoration
Ten_m	Gypsum based mortar	1040 ± 150 CE, Byzantine era
SecN5_mos	Gypsum based mortar	1560 ± 70 CE, Boniface of Ragusa Restoration
SecN3_m	Lime based mortar	1815 ± 32 CE, Komnenos Restoration
OM13	Proconnesos marble of variety type I	-
OM49	Proconnesos marble of variety type I	-
RC_wrs_left	Limestone, Holy Rock	-
SecN5_wrs	Limestone, Holy Rock	-
SecN3_wrs	Limestone, Holy Rock	-

2.2 SAMPLE PROCESSING AND DNA SEQUENCING

A non-invasive sampling process was adopted for the DNA extraction from all the samples under investigation. Material was collected with sterile cotton swabs and it was preserved in DNA/RNA protection buffer for safe transportation and preservation. DNA was extracted and its final concentration was measured for accurate quantification. Specifically, the DNA Extraction protocol included the following steps: (a) Sample stirring for 30 seconds using Vortex, (b) Removal of cotton swab from the vial, (c) buffer transfer to sterile ZR BashingBead Lysis Tubes (0.1 & 0.5 mm), (d) Extraction of genetic material (DNA) using the zymoBIOMICS DNA miniprep kit (Zymo Research, USA, cat # D4300) according to the manufacturer's instructions and (e) quantification and DNA quality control for each sample using the 1X dsDNA Assay Kit and the Qubit 4 Fluorometer (Thermo Fisher Scientific, USA).

Due to low DNA concentration in all extracted samples, the full-length 16S rRNA ribosomal gene was amplified with PCR. Equal amounts (ng) of PCR-amplified products with appropriate barcodes were pooled together in the preparation of a 16s sequencing library (Oxford Nanopore, UK), according to the manufacturer's recommendations. The sequencing library was loaded in an R9.4.1 flow cell on a MinION Mk1C (Oxford Nanopore, UK) and basecalling was performed with minKNOW software, while microbial communities were identified through an EPI2ME 16S analysis workflow software and proprietary bioinformatics pipelines. The software is based on Nextflow (DI Tommaso et al., 2017), which enables scalable and reproducible scientific workflows. The taxonomic classification accomplished with Centrifuge (Kim et al., 2016), a very rapid and in memory efficient system for classification of DNA sequences from microbial samples. The system uses a novel indexing scheme based on the Burrows-Wheeler transform (BWT) and the Ferragina-Manzini (FM) index, optimized specifically for the metagenomic classification problem. Centrifuge requires a relatively small index (e.g., 4.3 GB for ~4,100 bacterial genomes) yet provides very fast classification speed. The EPI2ME cloud-based software did not provide functionalities for statistical data evaluation. The taxonomic classification and quality of barcoded reads were downloaded in the form of a CSV file from the EPI2ME dashboard for further processing. This file included information on the sequencer run and further data such as read IDs, read accuracy, barcodes, and NCBI taxonomy IDs for classed reads. The CSV file was processed with python scripts for generating root level OTU tables, by matching NCBI taxa IDs to lineages and counting the number of reads per NCBI taxa ID. Further interpretation was facilitated by machine learning libraries and proprietary software, as well as by a multivariate, k mean clustering data analysis which was performed using ClustViz (Metsalu & Vilo, 2015), a widely used Bioinformatics web tool based on BoxPlotR and several R packages.

3. RESULTS & DISCUSSION

3.1 IDENTIFICATION & DESCRIPTION OF MICROBIAL COMMUNITIES

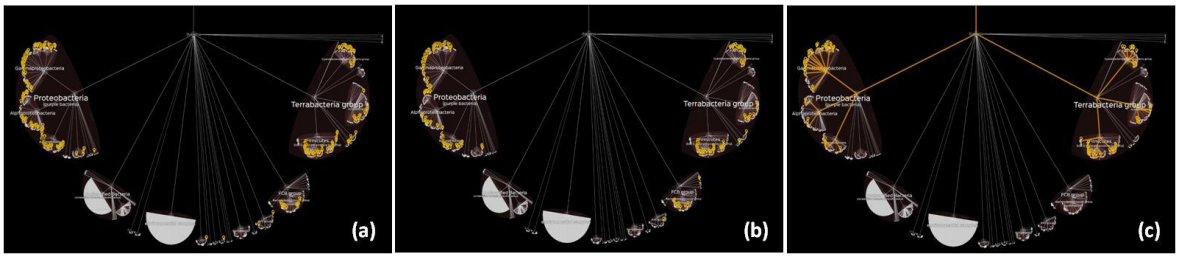

Figure 9. Taxonomic distribution of the microbial community composition; life maps of the Holy rock samples (a), the marble samples (b), and the mortar samples (c).

Regarding the taxonomic distribution of the microbial community in all the analyzed samples, it is noted that bacterial sequences represented 94.16% of the total sequences, whereas the other phyla presented were Eukaryota 4.19% (mostly the clade Opisthokonta, which includes metazoa and fungi) and Archaea 1.64%. The most abundant bacterial phyla are Proteobacteria, Terrabacteria, the Fibrobacteres-Chlorobi-Bacteroidetes (FCB) superphylum, the Planctomycetes-Verrucomicrobia-Chlamydiae (PVC) superphylum, Spirochaetes, while there is small fraction of unclassified bacteria. Within Proteobacteria, Gammaproteobacteria and Alphaproteobacteria are the most abundant classes.

Nanopore MinION-based metagenomic sequencing of long-read 16S rRNA amplicons generated a total of 2,408,076 sequence reads after quality control and basecalling. Based on sequencing data, DNA fragments of the expected length were successfully sequenced for all the samples under investigation. Microbial species can have high occupancy frequency within the host population for several reasons; for example, they can be common in the environment or diet (David et al., 2014), highly competitive against other microbes (Bauer et al., 2018; Coyte & Rakoff-Nahoum, 2019), or vertically transmitted colonizing a host (Funkhouser & Bordenstein, 2013). In most cases, identifying the underlying reason why some microbes have high frequency is difficult, and a microbe's occupancy frequency is not necessarily linked to its function or evolutionary history with the host (especially where host dependence is low), (Hammer et al., 2019).

Even though microbial presence has been investigated in a number of monuments and works of cultural heritage (Adamiak et al., 2018; Crispim et al., 2005; de Leo et al., 2012; Dyda et al., 2019; Mazzoli et al., 2018; Mihajlovski et al., 2017), this is the first time samples from the Holy Aedicule have been analysed for such findings with the result resolution offered by metagenomics. This comprehensive microbial presence documentation of selected samples of the monument can serve as a benchmark of the monument's state at the time of sampling and can therefore be used comparatively in any future microbial monitoring to reveal potential future biodeterioration, and therefore preservation needs, as well as potential influence of changes in the microenvironment of the monument.

Table II shows the results of the microbial identification in binary state (i.e. presence/absence), sorted by appearance frequency in the analyzed samples. It is observed that the microbial communities, developed on the examined samples, are characterized by different species in total, which belong to various genera; however, each sample demonstrates different number of species. In particular, OM-49 and Ten-m display the highest amounts of different species (161 and 150 species, respectively), while RC-wrs-left and SecN5-wrs follow regarding the abundance of species (147 and 142 species, respectively). Subsequently, SecN3-m, OM-13, SecN5-mos and SecN3-wrs demonstrate 104, 94, 93 and 91 species, respectively, while RC-m5 displays 83 species in total. Finally, 74 species are detected on Arc-m2, which presents the lowest amount of species compared to the rest of the examined samples.

Table II. Microbial communities identified per investigated sample by order of presence

Species	Arc-m2	OM-13	OM-49	RC-m5	RC-wrs-left	SecN3-m	SecN3-wrs	SecN5-mos	SecN5-wrs	Ten-m
Acinetobacter johnsonii	●	●	●	●	●	●	●	●	●	●
Azotobacter chroococcum	●	●	●	●	●	●	●	●	●	●
Chroococcidiopsis thermalis PCC 7203	●	●	●	●	●	●	●	●	●	●
Cutibacterium acnes	●	●	●	●	●	●	●	●	●	●
Loriellopsis cavernicola	●	●	●	●	●	●	●	●	●	●
Pseudomonas aeruginosa	●	●	●	●	●	●	●	●	●	●
Pseudomonas alcaligenes	●	●	●	●	●	●	●	●	●	●
Pseudomonas fulva	●	●	●	●	●	●	●	●	●	●
Pseudomonas guariconensis	●	●	●	●	●	●	●	●	●	●
Pseudomonas guguanensis	●	●	●	●	●	●	●	●	●	●
Pseudomonas hydrolytica	●	●	●	●	●	●	●	●	●	●
Pseudomonas knackmussii B13	●	●	●	●	●	●	●	●	●	●
Pseudomonas nitroreducens	●	●	●	●	●	●	●	●	●	●
Pseudomonas otitidis	●	●	●	●	●	●	●	●	●	●
Pseudomonas plecoglossicida	●	●	●	●	●	●	●	●	●	●
Pseudomonas putida	●	●	●	●	●	●	●	●	●	●
Pseudomonas resinovorans	●	●	●	●	●	●	●	●	●	●
Pseudomonas stutzeri	●	●	●	●	●	●	●	●	●	●
Pseudomonas stutzeri ATCC 17588 = LMG 11199	●	●	●	●	●	●	●	●	●	●
Staphylococcus saccharolyticus	●	●	●	●	●	●	●	●	●	●
Zhihengliuella somnathii	●	●	●	●	●	●	●	●	●	●
Pseudomonas mangrovi	●	●	●	●	●	●	●		●	●
Pseudomonas oryzihabitans	●	●	●	●	●	●	●		●	●
Aliterella antarctica	●	●	●	●	●	●		●	●	●
Pseudomonas glareae	●	●	●	●	●		●	●	●	●
Pseudomonas khazarica	●	●	●	●	●		●	●	●	●
Pseudomonas oleovorans	●	●	●	●	●		●	●	●	●
Acinetobacter chinensis	●	●	●		●	●	●	●	●	●
Acinetobacter tjernbergiae		●	●	●	●	●	●	●	●	●
Pseudomonas aestus	●	●	●	●	●	●			●	●
Pseudomonas citronellolis	●	●	●	●	●	●			●	●
Staphylococcus epidermidis	●	●	●	●	●		●	●	●	
Pseudomonas monteilii	●	●	●	●	●		●		●	●
Pseudomonas oceani	●	●	●	●	●		●		●	●
Pseudomonas sagittaria	●	●	●	●		●	●		●	●
Pseudomonas mendocina	●	●	●	●		●		●	●	●
Pseudomonas urumqiensis	●	●	●	●		●		●	●	●
Trichocoleus desertorum	●		●	●	●	●		●	●	●
Pseudomonas reidholzensis		●	●	●	●	●	●	●		●

Species	Arc-m2	OM-13	OM-49	RC-m5	RC-wrs-left	SecN3-m	SecN3-wrs	SecN5-mos	SecN5-wrs	Ten-m
Acinetobacter haemolyticus		●	●	●	●	●	●		●	●
Marinobacter lutaoensis		●	●	●	●	●	●		●	●
Acinetobacter bouvetii		●	●	●	●	●		●	●	●
Acinetobacter baumannii		●	●	●	●		●	●	●	●
Potamolinea aerugineo-caerulea		●	●		●	●	●	●	●	●
Massilia aurea			●	●	●	●	●	●	●	●
Staphylococcus capitis subsp. urealyticus	●	●	●	●	●				●	●
Pseudomonas amygdali	●	●	●	●			●		●	●
Pseudomonas benzenivorans	●	●	●	●			●		●	●
Cylindrospermum stagnale	●	●	●	●				●	●	●
Pseudomonas argentinensis	●	●	●	●				●	●	●
Pseudomonas indica	●	●	●	●				●	●	●
Stanieria cyanosphaera PCC 7437	●	●	●	●				●	●	●
Acaryochloris marina MBIC11017	●		●		●	●		●	●	●
Ralstonia syzygii	●		●		●	●		●	●	●
Staphylococcus hominis		●	●	●	●	●		●	●	
Pseudomonas multiresinivorans		●	●	●	●	●		●		●
Microbulbifer salipaludis		●	●	●	●	●			●	●
Pseudomonas chengduensis		●	●	●		●	●		●	●
Pseudomonas flavescens		●	●	●		●	●		●	●
Comamonas denitrificans		●	●		●	●		●	●	●
Comamonas nitrativorans		●	●		●	●		●	●	●
Rehaibacterium terrae		●	●		●	●		●	●	●
Acinetobacter schindleri		●	●			●	●	●	●	●
Acinetobacter equi			●		●	●	●	●	●	●
Acinetobacter junii			●		●	●	●	●	●	●
Acinetobacter proteolyticus			●		●	●	●	●	●	●
Comamonas phosphati			●		●	●	●	●	●	●
Pseudomonas peli	●	●	●	●		●				●
Anabaena cylindrica PCC 7122	●	●	●	●					●	●
Staphylococcus devriesei	●	●	●		●	●			●	
Aeromonas hydrophila	●	●	●		●		●		●	
Pseudomonas pohangensis	●	●	●		●		●			●
Crinalium epipsammum	●	●	●		●			●	●	
Aeromonas enteropelogenes	●	●			●		●		●	●
Staphylococcus croceilyticus	●		●	●	●	●			●	
Coleofasciculus chthonoplastes	●		●	●	●			●	●	
Oscillatoria nigro-viridis	●		●	●		●			●	●
Synechococcus elongatus PCC 6301	●		●		●	●		●	●	
Arthrospira platensis	●		●		●			●	●	●

Table II. Microbial communities identified per investigated sample by order of presence (continuing)

Species	Arc-m2	OM-13	OM-49	RC-m5	RC-wrs-left	SecN3-m	SecN3-wrs	SecN5-mos	SecN5-wrs	Ten-m
Kastovskya adunca	●		●		●			●	●	●
Acinetobacter albensis	●		●			●	●		●	●
Ralstonia pickettii	●		●			●		●	●	●
Aerosakkonema funiforme	●				●	●		●	●	●
Staphylococcus caprae		●	●	●	●	●				●
Pseudomonas formosensis		●	●	●			●		●	●
Moraxella osloensis		●	●		●	●		●		●
Acinetobacter calcoaceticus		●	●		●	●			●	●
Escherichia fergusonii ATCC 35469		●	●			●		●	●	●
Massilia timonae		●			●	●	●	●		●
Citrobacter murliniae			●	●	●	●			●	●
Acinetobacter variabilis			●	●	●		●	●		●
Cephalothrix komarekiana CCIBt 3277			●	●	●			●	●	●
Comamonas testosteroni			●		●	●	●		●	●
Leclercia adecarboxylata			●		●	●	●		●	●
Delftia acidovorans			●		●		●	●	●	●
Pseudomonas hussainii	●	●		●		●				●
Pseudomonas oryzae	●	●		●				●		●
Gloeobacter violaceus PCC 7421	●		●	●				●		●
Rheinheimera sediminis	●		●		●	●	●			
Acinetobacter seohaensis	●		●		●			●	●	
Pseudomonas punonensis		●	●	●					●	●
Acinetobacter tandoii		●	●			●			●	●
Shigella flexneri		●	●			●			●	●
Shigella sonnei		●	●			●			●	●
Arcobacter cryaerophilus		●	●					●	●	●
Pantoea allii		●		●		●			●	●
Hydrogenophaga taeniospiralis		●				●	●		●	●
Methylomonas methanica			●	●	●			●		●
Streptococcus mitis			●	●		●		●		●
Acinetobacter lwoffii			●	●		●			●	●
Acidovorax temperans			●	●			●		●	●
Priestia flexa			●		●	●		●		●
Alkanindiges illinoisensis			●		●	●			●	●
Comamonas jiangduensis			●		●		●		●	●
Duganella qianjiadongensis			●		●		●		●	●
Enterobacter cancerogenus			●		●		●		●	●
Chiayiivirga flava			●		●			●	●	●
Paracraurococcus ruber			●		●			●	●	●
Acinetobacter radioresistens			●			●	●		●	●
Comamonas terrigena			●			●	●		●	●
Psychrobacter faecalis			●				●	●	●	●

Species	Arc-m2	OM-13	OM-49	RC-m5	RC-wrs-left	SecN3-m	SecN3-wrs	SecN5-mos	SecN5-wrs	Ten-m
Staphylococcus saprophyticus subsp. saprophyticus ATCC 15305 = NCTC 7292	●		●		●			●		
Ralstonia solanacearum	●		●			●			●	
Staphylococcus pasteuri		●	●			●			●	
Massilia atriviolacea			●	●	●		●			
Pararheinheimera soli			●	●	●			●		
Staphylococcus warneri			●	●		●			●	
Neosynechococcus sphagnicola			●		●			●	●	
Acinetobacter oleivorans			●		●				●	●
Enterobacter mori			●			●	●			●
Pseudomonas migulae			●			●			●	●
Pseudomonas weihenstephanensis			●			●			●	●
Ralstonia mannitolilytica			●			●			●	●
Thermomonas carbonis			●			●			●	●
Brevundimonas naejangsanensis			●				●		●	●
Brevundimonas nasdae			●				●		●	●
Pectobacterium aroidearum			●					●	●	●
Stenotrophomonas maltophilia			●					●	●	●
Janthinobacterium rivuli					●	●	●	●		
Microbacterium sediminis					●	●		●	●	
Absiella tortuosum					●			●	●	●
Rhodanobacter lindaniclasticus	●		●		●					
Aeromonas jandaei	●		●							●
Aeromonas taiwanensis	●		●							●
Janthinobacterium violaceinigrum	●				●		●			
Staphylococcus edaphicus		●	●		●					
Atlantibacter hermannii		●	●					●		
Escherichia marmotae		●	●						●	
Pantoea agglomerans		●				●				●
Thiohalobacter thiocyanaticus		●							●	●
Massilia dura			●		●		●			
Massilia glaciei			●		●		●			
Massilia putida			●		●		●			
Klebsiella aerogenes KCTC 2190			●		●					●
Sphingobacterium mizutaii			●		●					●
Staphylococcus aureus			●			●		●		
Streptococcus thermophilus			●			●			●	
Cohnella faecalis			●			●				●
Comamonas aquatica subsp. rana			●				●			●
Uliginosibacterium paludis			●					●	●	
Delftia lacustris			●						●	●
Stenotrophomonas rhizophila			●						●	●
Massilia agri				●	●		●			

Table II. Microbial communities identified per investigated sample by order of presence (continuing)

Species	Arc-m2	OM-13	OM-49	RC-m5	RC-wrs-left	SecN3-m	SecN3-wrs	SecN5-mos	SecN5-wrs	Ten-m
Pseudomonas protegens				•					•	•
Massilia aquatica					•	•	•			
Massilia brevitalea					•	•	•			
Massilia namucuonensis					•	•	•			
Massilia yuzhufengensis					•	•	•			
Janthinobacterium lividum					•		•	•		
Massilia oculi					•		•		•	
Duganella albus					•		•			•
Pseudidiomarina maritima					•			•	•	
Rhodocyclus purpureus					•			•	•	
Polaromonas hydrogenivorans					•			•		•
Bacillus nealsonii					•				•	•
Metabacillus niabensis					•				•	•
Acidovorax defluvii						•			•	•
Limnohabitans parvus II-B4								•	•	•
Bacillus cereus	•				•					
Enterobacter cloacae		•	•							
Metakosakonia massiliensis JC163		•	•							
Escherichia albertii		•							•	
Mixta intestinalis		•								•
Rhodanobacter caeni			•		•					
Paracoccus chinensis			•			•				
Pararheinheimera mesophila			•				•			
Giesbergeria voronezhensis			•					•		
Lactococcus piscium			•					•		
Rhodobacter thermarum			•							•
Serratia oryzae			•							•
Rubellimicrobium roseum				•	•					
Noviherbaspirillum suwonense				•			•			
Kocuria atrinae				•						•
Limnochorda pilosa				•						•
Salinicoccus kekensis					•	•				
Bacillus mannanilyticus					•		•			
Duganella fentianensis					•		•			
Frigoribacterium endophyticum					•		•			
Massilia chloroacetimidivorans					•		•			
Pseudomonas gessardii					•				•	
Aeromonas media									•	•
Azospira oryzae PS									•	•
Deinococcus murrayi		•								
Knoellia locipacati		•								
Pedomicrobium americanum		•								
Amaricoccus macauensis			•							
Kocuria rhizophila			•							

Species	Arc-m2	OM-13	OM-49	RC-m5	RC-wrs-left	SecN3-m	SecN3-wrs	SecN5-mos	SecN5-wrs	Ten-m
Leucobacter alluvii			•							
Anaerococcus nagyae					•					
Anaerococcus urinomassiliensis					•					
Aquincola tertiaricarbonis					•					
Arthrobacter agilis					•					
Deinococcus hopiensis KR-140					•					
Deinococcus oregonensis					•					
Devosia submarina					•					
Exiguobacterium acetylicum					•					
Hymenobacter chitinivorans					•					
Hymenobacter gummosus					•					
Hymenobacter knuensis					•					
Hymenobacter luteus					•					
Hymenobacter monticola					•					
Hymenobacter psychrotolerans					•					
Hymenobacter swuensis DY53					•					
Hymenobacter tibetensis					•					
Methylobacterium hispanicum					•					
Rhodocytophaga aerolata					•					
Rubellimicrobium rubrum					•					
Saccharibacillus qingshengii					•					
Salinicoccus qingdaonensis					•					
Sphingomonas fonticola					•					
Tsuneonella rigui					•					
Gluconacetobacter liquefaciens						•				
Neisseria sicca ATCC 29256							•			
Aromatoleum buckelii									•	
Erwinia persicina									•	
Streptococcus oralis ATCC 35037									•	
Aquabacterium parvum										•
Planococcus dechangensis										•
Propionivibrio limicola										•
Stenotrophomonas koreensis										•

Furthermore, it is observed that some species showed to be present in multiple samples. In fact, 21 species are omnipresent in all the examined samples, which is the 8.75% of the totally detected species. It is noticed that many species of the genus *Pseudomonas* are dominant in all the examined samples and specifically the species *Pseudomonas aeruginosa, Pseudomonas alcaligenes, Pseudomonas fulva, Pseudomonas guariconensis, Pseudomonas guguanensis, Pseudomonas hydrolytica, Pseudomonas knackmussii B13, Pseudomonas nitroreducens, Pseudomonas otitidis, Pseudomonas plecoglossicida, Pseudomonas putida, Pseudomonas resinovorans, Pseudomonas stutzeri* and *Pseudomonas stutzeri ATCC 17588 = LMG 11199*. Members of other genera are detected in all the investigated samples, as well. These are the species *Acinetobacter johnsonii, Azotobacter chroococcum, Chroococcidiopsis thermalis PCC 7203, Cutibacterium acnes, Loriellopsis cavernicola, Staphylococcus saccharolyticus,* and *Zhihengliuella somnathii*.

Concerning the presence of the common species in relation to the total ones per examined sample, it is observed that Arc-m2 demonstrates the highest percentage (28.38%) of common species, while RC-m5 displays the second higher percentage (25.30%). Subsequently, SecN3-wrs, SecN5-mos and OM-13 follow, regarding the percentage of species that are detected in all the investigated samples, with 23.08%, 22.58% and 22.34%, respectively. SecN3-m and SecN5-wrs also present high percentages of species that are omnipresent in all the investigated samples (20.19% and 14.79%, respectively), while RC-wrs-left, Ten-m and OM-49 demonstrate the lowest corresponding percentages (14.79%, 14.00% and 13.04%, respectively). Finally, it is worth noting that there are several species that are detected in 2 to 9 of the examined samples and belong to various genera, such as *Massilia aurea, Staphylococcus hominis, Escherichia fergusonii* ATCC 35469 and *Chiayiivirga flava* (Table II).

Apart from the species that are present in multiple samples, there are 38 species that are uniquely detected in some samples and are the 15.83% of the totally identified species. RC-wrs-left demonstrates the highest amount of the uniquely detected species, while it is observed that species of the genus *Hymenobacter* are mostly present in this sample. Similarly, OM-13, Ten-m, SecN3-wrs, OM-49, SecN5-wrs, SecN3-m also contain species that are uniquely identified and belong to several genera. Finally, among the examined samples, Arc-m2, RC-m5, SecN5-mos do not demonstrate species that are uniquely identified.Regarding the percentages of the uniquely detected species, in relation to the total ones, per sample, it is noticed that RC-wrs-left demonstrates not only the highest amount, but also the highest percentage of these species, which is 15.65%. OM-13, Ten-m and SecN5-wrs follow by percentage value order, with 3.19%, 2.67% and 2.11%, respectively. Subsequently, OM-49, SecN3-wrs and SecN3-m display lower percentages of the species that are individually detected, while the latters are presented by 1.86%, 1.10% and 0.96%, respectively. Finally, as it is above mentioned, Arc-m2, RC-m5, SecN5-mos do not demonstrate uniquely identified species.

All further analysis focused on the relative abundances of microbial presence in each species, as this metric is more reliable than absolute read count, which is dependent on the sampling procedure. In particular, the most abundant species per sample are illustrated in figure 10 and presented in Table III.

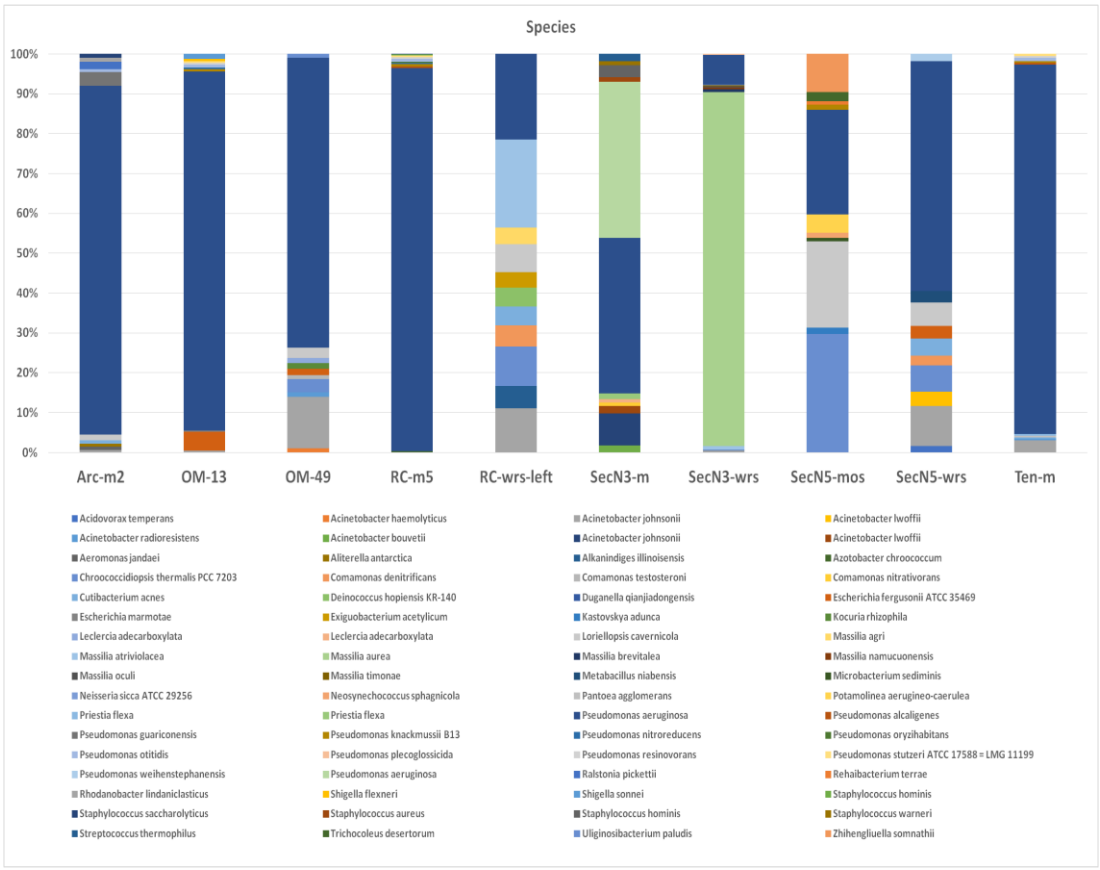

Figure 10. Bar chart showing the most abundant microbial communities for each sample

Table III. Summary of the most abundant microbial presence per investigated sample

Sample Code	Species & their relative abundance (%)
Arc_m2	*Pseudomonas aeruginosa* (77.8%); *Pseudomonas guariconensis* (3.08%); *Ralstonia pickettii* (1.6%); *Loriellopsis cavernicola* (1.28%); *Rhodanobacter lindaniclasticus* (0.95%); *Staphylococcus saccharolyticus* (0.8%); *Cutibacterium acnes* (0.75%); *Aeromonas jandaei* (0.68%); *Aliterella Antarctica* (0.65%); *Pseudomonas otitidis* (0.65%); *Acinetobacter johnsonii* (0.58%);
RC_m5	*Pseudomonas aeruginosa* (92.35%); *Pseudomonas otitidis* (0.78%); *Pseudomonas knackmussii* B13 (0.52%); *Pseudomonas stutzeri ATCC 17588* (0.48%); *Pseudomonas alcaligenes* (0.42%); *Pseudomonas resinovorans* (0.34%); *Azotobacter chroococcum* (0.30%); *Pseudomonas nitroreducens* (0.29%); *Pseudomonas oryzihabitans* (0.22%); *Staphylococcus hominis* (0.17%); *Staphylococcus saccharolyticus* (0.15%);
Ten_m	*Pseudomonas aeruginosa* (81.18%); *Acinetobacter johnsonii* (2.61%); *Pseudomonas otitidis* (0.76%); *Pseudomonas stutzeri* ATCC 17588 (0.46%); *Pseudomonas alcaligenes* (0.43%); *Priesta flexa* (0.43%); *Pseudomonas knackmussii* B13 (0.42%); *Actinobacter radioresistens* (0.40%); *Cutibacterium acnes* (0.34%); *Pantoea agglomerans* (0.33%); *Pseudomonas resinovorans* (0.32);
SecN5_mos	*Chroococcidiopsis thermalis* PCC 7203 (16.08%); *Pseudomonas aeruginosa* (14.2%); *Loriellopsis cavernicola* (11.75%); *abundance*(5.15%); *Potamolinea aerugineo-caerulea* (2.5%); *Trichocoleus desertorum* (1.28%); *Kastovskya adunca* (0.83%); *Pseudomonas knackmussii* B13 (0.7%); *Neosynechococcus sphagnicola* (0.68%); *Microbacterium sediminis* (0.45%); *Rehaibacterium terrae* (0.43%);
SecN3_m	*Pseudomonas aeruginosa* (38.5%); *Acinetobacter johnsonii* (7.9%); *Staphylococcus hominis* (2.95%); *Acinetobacter lwoffii* (1.90%); *Streptococcus thermophilus* (1.85%); *Acinetobacter bouvetii* (1.70%); *Priestia flexa* (1.40%); *Staphylococcus aureus* (1.25%); *Staphylococcus warneri* (0.90%); *Leclercia adecarboxylata* (0.85%); *Comamonas nitrativorans* (0.85%); *Pseudomonas chengduensis*(0.85%);
OM13	*Pseudomonas aeruginosa* (84.6%); *Escherichia fergusonii* ATCC 35469 (4.4%); *Shigella sonnei* (1.19%); *Pseudomonas otitidis* (0.71%); *Pseudomonas knackmussii* B13 (0.58%); *Shigella flexneri* (0.51%); *Pseudomonas stutzeri* ATCC 17588 (0.47%); *Acinetobacter johnsonii* (0.44%); *Pseudomonas resinovorans* (0.35%); *Escherichia marmotae* (0.33%); *Pseudomonas nitroreducens* (0.30%);

OM49	*Pseudomonas aeruginosa* (47.6%); *Acinetobacter johnsonii* (8.49%); *Chroococcidiopsis thermalis* PCC 7203 (2.13%); *Loriellopsis cavernicola* (1.6%); *Kocuria rhizophila* (1.01%); *Escherichia fergusonii* ATCC 35469 (0.99%); *Leclercia adecarboxylata* (0.86%); *Acinetobacter radioresistens* (0.76%); *Comamonas testosterone* (0.69%); *Uliginosibacterium paludis* (0.67%); *Acinetobacter haemolyticus* (0.64%)
RC_wrs_left	*Massilia atriviolacea* (10.86%); *Pseudomonas aeruginosa* (10.56%); *Acinetobacter johnsonii* (5.46%); *Chroococcidiopsis thermalis* PCC 7203 (4.87%); *Loriellopsis cavernicola* (3.48%); *Alkanindiges illinoisensis* (2.75%); *Comamonas denitrificans* (2.63%); *Cutibacterium acnes* (2.34%); *Deinococcus hopiensis KR-140* (2.3%); *Massilia agri* (2.03%); *Exiguobacterium acetylicum* (1.91%);
SecN5_wrs	*Pseudomonas aeruginosa* (32.78%); *Acinetobacter johnsonii* (6.93%); *Chroococcidiopsis thermalis* PCC 7203 (3.78%); *Loriellopsis cavernicola* (3.28%); *Cutibacterium acnes* (2.45%); *Acinetobacter lwoffii* (2.0%); *Escherichia fergusonii* ATCC 35469 (1.85%); *Metabacillus niabensis* (1.65%); *Comamonas denitrificans* (1.35%); *Pseudomonas weihenstephanensis* (1.05%); *Acidovorax temperans* (0.9%);
SecN3_wrs	*Massilia aurea* (85.43%); *Pseudomonas aeruginosa* (7.27%); *Massilia atriviolacea* (0.97%); *Massilia brevitalea* (0.71%); *Massilia namucuonensis* (0.43%); *Acinetobacter johnsonii* (0.42%); *Massilia oculi* (0.29%); *Pseudomonas plecoglossicida* (0.19%); *Duganella qianjiadongensis* (0.19%); *Neisseria sicca* ATCC 29256 (0.16%); *Massilia timonae* (0.15%); *Massilia putida* (0.15%);

According to Table III, it is observed that core bacterial microbiome identification for the most abundant species is composed of a wide range of species from several genera. A few representatives from the genera *Pseudomonas, Acinetobacter, Chroococcidiopsis, Loriellopsis, Zhihengliuella, Massilia, Staphylococcus, Comamonas* and *Escherichia* showed to be present in all the examined samples displaying high relative abundances. In particular, *Pseudomonas aeruginosa, Acinetobacter johnsonii, Chroococcidiopsis thermalis PCC 7203, Loriellopsis cavernicola, Zhihengliuella somnathii, Massilia atriviolacea* and *Massilia aurea* demonstrate the highest relative abundances in the examined samples compared to the rest of the identified species.

Extending the observation scope to the whole dataset, it is noticed that one microorganism that stands out as members of its genus detected in all samples is *Pseudomonas aeruginosa*. A universally spread species, *P. aeruginosa* is prevelant in RC-m5 (92.35%), while OM13, Ten-m and Arc_m2 follow, regarding the relative abundances, with 84.59%, 81.18% and 77.75%, respectively. OM49, SecN3-m, SecN5-wrs, SecN5-mos and RC-wrs-left are characterized by lower relative abundances of this species, whereas SecN3-wrs demonstrates the lowest relative abundance regarding the *Pseudomonas aeruginosa* presence. Subsequently, *Acinetobacter johnsonii* is detected in 8 examined specimens and particularly in Arc-m2, OM-13, OM-49, RC-wrs-left, SecN3-m, SecN5-wrs, SecN3-wrs, Ten-m, while OM-49 and SwcN3-m display the highest relative abundances (8.49% and 7.90%, respectively). *Loriellopsis cavernicola* is also detected in Arc-m2, OM-49, RC-wrs-left, SecN5-wrs and SecN5-mos with high relative abundances, while the highest one is presented in SecN5-mos (11.75%). Subsequently, OM-49, RC-wrs-left, SecN5-wrs and SecN5-mos are colonized by *Chroococcidiopsis thermalis PCC 7203,* which is most abundant in SecN5-mos and RC-wrs-left (16.08% and 4.86%, respectively). It is worth mentioning that *Comamonas denitrificans* is identified only in RC-wrs-left and SecN5-wrs, but with comparable abundances and particularly with 2.63% and 1.35%, respectively. Moreover, *Staphylococcus hominis* is detected only in 2 samples and specifically in SecN3-m (2.95%) and RC-m5 (0.17%). Finally, some more species are also detected in multiple samples, which though display lower relative abundances. These are the species *Cutibacterium acnes* (in samples Arc-m2, RC-wrs-left, SecN5-wrs and Ten-m), *Pseudomonas alcaligenes* (in samples RC-m5 and Ten-m 2), *Pseudomonas knackmussii B13* (in samples OM-13, RC-m5, SecN5-mos and Ten-m), *Pseudomonas nitroreducens* (in samples OM-13 and RC-m5), *Pseudomonas otitidis* (in samples Arc-m2, OM-13, RC-m5 and Ten-m), *Pseudomonas resinovorans* (in samples OM-13, RC-m5 and Ten-m), *Pseudomonas stutzeri ATCC 17588 = LMG 11199* (in samples OM-13, RC-m5 and Ten-m), *Staphylococcus saccharolyticus* (in samples Arc-m2 and RC-m5), *Escherichia fergusonii ATCC 35469* (in samples OM-13, OM-49 and SecN5-wrs) and *Acinetobacter radioresistens* (in samples OM-49 and Ten-m).

Concerning the common microbial communities developed in each material, it is observed that marble samples (OM-13 and OM-49) demonstrate only 3 common species, which are the *Pseudomonas aeruginosa, Acinetobacter johnsonii* and *Escherichia fergusonii ATCC 35469.* It is worth noting that *Pseudomonas aeruginosa* is the most dominant in both marble samples, whereas *Escherichia fergusonii ATCC 35469* abundance is higher in OM-13 and *Acinetobacter johnsonii* abundance is higher in OM-49. Furthermore, OM-13 is colonized by

Pseudomonas knackmussii B13, Pseudomonas nitroreducens, Pseudomonas otitidis, Pseudomonas resinovorans and *Pseudomonas stutzeri ATCC 17588 = LMG 11199,* which are characterized by low relative abundances. On the contrary, *Chroococcidiopsis thermalis PCC 7203* and *Loriellopsis cavernicola* are detected individually in OM-49.

As far as it concerns the limestones sampled from the Holy rock (RC-wrs-left, SecN5-wrs and SecN3-wrs), it is observed that they demonstrate only 2 common species, which are the *Pseudomonas aeruginosa* and *Acinetobacter johnsonii*, while the former is more dominant compared to the latter in the investigated Holy rock samples. It is worth noting that, except for the aforementioned common species, SecN3-wrs also presents the species *Massilia aurea,* which is detected with the highest relative abundance in this sample. Subsequently, *Chroococcidiopsis thermalis PCC 7203, Cutibacterium acnes, Loriellopsis cavernicol* and *Comamonas denitrificans* are detected with comparable abundances both in RC-wrs-left and SecN5-wrs, while *Escherichia fergusonii ATCC 35469* is only present in SecN5-wrs. Finally, *Massilia atriviolacea* showed to be the most dominant species only in RC-wrs-left.

Regarding the mortar samples, it is noticed that only *Pseudomonas aeruginosa* is universally detected and demonstrates high relative abundances. Among the mortar samples, SecN3-m, that is the only lime-based mortar as all the rest are gypsum based, is colonized by another 2 common species, which are the *Acinetobacter johnsonii* and *Staphylococcus hominis*, as well as it displays several uniquely detected species, such as *Acinetobacter lwoffii, Streptococcus thermophiles, Acinetobacter bouvetii, Priestia flexa* and *Staphylococcus aureus,* which are identified with comparable abundances. It is also evident that *Acinetobacter johnsonii* demonstrates the highest relative abundance in SecN3-m comparing to the rest of the mortar samples, which could be attributed to the different chemical composition of this sample. Among the gypsum-based mortars, it is worth noting that SecN5-mos is the only mortar that is colonized by *Chroococcidiopsis thermalis PCC 7203*, which is the most dominant species in this sample, as well as it demonstrates uniquely detected species, such as *Zhihengliuella somnathii, Potamolinea aerugineo-caerulea* and *Trichocoleus desertorum*. Moreover, SecN5-mos exhibits the highest relative abundances of *Loriellopsis cavernicola,* which is also identified in Arc-m2. Concerning Arc-m2, apart from the aforementioned common species, it also displays the species *Cutibacterium acnes, Pseudomonas otitidis* and *Staphylococcus saccharolyticus* with a low relative abundance, whereas it is colonized by the uniquely detected species *Pseudomonas guariconensis,* as well. Finally, RC-m5 and Ten-m demonstrate the highest relative abundances regarding the *Pseudomonas aeruginosa* presence, as well as they exhibit the highest amounts of the common species (9 common species in each mortar sample) compared to the rest mortar samples. Both RC-m5 and Ten-m are colonized by *Pseudomonas alcaligenes, Pseudomonas knackmussii B13, Pseudomonas otitidis, Pseudomonas resinovorans, Pseudomonas stutzeri ATCC 17588 = LMG 11199,* whereas *Pseudomonas nitroreducens, Staphylococcus saccharolyticus* and *Staphylococcus hominis* are detected in RC-m5 and *Acinetobacter johnsonii, Cutibacterium acnes* and *Acinetobacter radioresistens* are identified in Ten-m; however all the aforementioned species showed to be present with low relative abundances.

Finally it is observed that all the investigated samples present from 4 (SecN5-mos) to 9 (RC-m5 and Ten-m) common species with comparable relative abundances, except for the samples SecN3-m and SecN3-wrs, which differ and present only 2 common species (*Pseudomonas aeruginosa* and *Acinetobacter johnsonii*).

A few abundant microbes, as well as a few interesting species in terms of biological and functional characteristics are summarized below:

Pseudomonas aeruginosa. P. aeruginosa is an extremely widespread (Mazzoli et al., 2018), environmental bacterium characterized by its ability to attach to surfaces and form bacterial biofilms. A large number of metabolic pathways and regulatory genes make this bacterium highly adaptive to various growth conditions, with the requirement of aerobic growth. P. aeruginosa has been isolated from a wide range of material such as stainless steel, polymers, fresco paintings and several types of fabric where it was linked to biodeterioration processes (Gu, 2007; Mazzoli et al., 2018; Zhou et al., 2018). The ability to form biofilm on stone is also well established and its ability to produce extracellular polymeric substances (EPS) protects the micro-organism from biocides, enhancing its biofilm-forming capacity (Kwiatkowski & Löfvendahl, 2005).

Chroococcidiopsis thermalis PCC 7203. The extremophile Chroococcidiopsis thermalis, belonging to the phylum Cyanobacteria, is known to be rock-inhabiting cyanobacteria (McNamara et al., 2006). Cyanobacteria are Gram-negative bacteria that obtain energy via photosynthesis. They are photolithoautotrophs, and have repeatedly been found in a wide variety of terrestrial and rock habitats including limestone, hard granite, gypsum, sandstone (De Los Ríos et al., 2007), stone monuments, building surfaces (Crispim & Gaylarde, 2005). Found in abundance in both endolithic and epilithic ecosystems, cyanobacteria are characterized by their ability to resist desiccation or froze in extreme environments such as hot or cold desserts (Wynn-Williams, 2006). It is considered that the microbial colonization starts with biofilm formation on the stone surface built by phototrophic organisms such as Cyanobacteria, algae or mosses. In porous material, such as rock or limestone, the biofilm penetrates to the inner surface favoring endolithic microbial colonization. Through several chemical and physical biodeterioration processes these organisms can potentially corrupt the structure of the rock material and contribute to degradation of cultural heritage (Crispim & Gaylarde, 2005; McNamara et al., 2006).

Loriellopsis cavernicola. This cyanobacteria representative was first isolated from a Spanish cave in 2011 (Lamprinou et al., 2011). It has since been isolated from quartz, white carbonate and marble rock types at the Mojave Desert which is considered to be a terrestrial analogue to Mars in many geological and astrobiological aspects (Smith et al., 2014). L. cavernicola was detected as visible hypolithic growth, which can be explained as all analyzed rock types are translucent. Epilithic presence of L. cavernicola was also detected on the stone wall of the royal abbey of Chaalis and specifically at a discolored part of the wall (Mihajlovski et al., 2017).

Massilia aurea. This strictly aerobic species of the genus Massilia produces yellow-pigmented colonies and was first isolated from drinking water in Spain (Gallego et al., 2006). There are only few mentions of this species in the literature, but genetically close species have mainly been found in air and soil samples including soil from the Tibetan plateau (Weon et al., 2008; Zhang et al., 2020; Zul et al., 2008).

Acinetobacter johnsonii. The species Acinetobacter johnsonii is a carbonatogenic bacterium that is commonly found in Mediterranean calcareous stones and shows a high capacity to induce calcium carbonate precipitation on decayed stones (Jroundi et al., 2017). It has also been detected in biofilm formations in calcareous cave walls, demonstrating a close association between bacterial metabolism and calcification process, resulting in mineral deposits and modification of the cave environment (Banerjee & Joshi, 2014).

Pantoea agglomerans. An ubiquitous bacterium commonly isolated from plant surfaces, seeds, fruit, and animal or human feces. It has been claimed that in one case the bacterium was traced in a possibly smuggled ancient marble statue, subjected to molecular analysis, in order to reconstruct the history of its storage (Piñar et al., 2019). Pantoea agglomerans has, also been isolated from specimens taken from ancient marble quarry (Penteli mountain), and has been reported as candidate for bioconsolidation and biorestoration strategies aiming at the preservation of stone monuments due to their ability to induce calcium carbonate precipitation (Daskalakis et al., 2013). Yet, due to its functional versatility, the presence of P. agglomerans might be attributed to multiple origins.

Zhihengliuella somnathii. A halotolerant actinobacterium isolated from the rhizosphere of Salicornia brachiata, an extreme halophyte. This species is able to tolerate high concentrations of NaCl (Jha et al., 2015).

Kocuria rhizophila. A halotolerant, actinobacterium isolated from the rhizosphere of narrowleaf cattail (Typha angustifolia). Members of the genus Kocuria were isolated from a wide variety of natural sources including mammalian skin, soil, the rhizosphere, fermented foods, clinical specimens, freshwater and marine sediments, suggesting a high adaptation to variant ecological niches (Takarada et al., 2008).

Comamonas denitrificans. Comamonas denitrificans is a denitrifying Proteobacterium isolated from activated sludge (Gumaelius et al., 2001). A member of the Comamonas genus (C. testosteroni) has previously been shown to be a good candidate for concrete and graphite surface biocleaning (Sanmartín et al., 2021).

Exiguobacterium acetylicum. Belonging to the phylum Firmicutes, the genus Exiguobacterium includes extremophile strains (-12-55 °C) found in a variety of environments such as soil, water, permafrost, rhizosphere, marine fish, biofilms (Vishnivetskaya et al., 2009). Some lineages of the genus are known to be metal-resistant and plant growth promoters that can be used as bioinoculants for contaminated soil remediation and phytotoxicity reducers (Benef. Microbes Agro-Ecology, 2020).

Salinicoccus qingdaonensis. S. qingdaonensis are moderately halophilic and heterotrophic cocci found in salt rich environments such as fermented food, solar salterns, salt mines, salt lake, saline soils (Hyun et al., 2013), desert soils and soda lakes (Kiledal et al., 2021). All type strains of Salinicoccus species are halotolerant, where 2-20% NaCl concentrations were suitable for growth (Hyun et al., 2013).

Staphylococcus hominis. Heterotrophic bacterial species, common in human flora (Kloos & Schleifer, 1975). It has been detected in both damaged and undamaged surfaces of antique limestone buildings (Skipper, 2018). Also, it has been isolated from biodeteriorated surfaces (whitish/grey patinas with no apparent cyanobacteria colonization) of the catacombs of St. Callistus in Rome (de Leo et al., 2012), most likely of anthropogenic origins.

Chiayiivirga flava. Mesophilic Proteobacteria members of the genus Rhodanobacteraceae. C. flava shows low tolerance to NaCl (0-2%) and has been isolated from agricultural soil specimens from Taiwan (Hsu et al., 2013).

It is worth mentioning that the halotolerant actinobacterium *Zhihengliuella somnathii* is detected in all the samples under investigation, while it is found in abundance in the mortar sample SecN5_mos. Other halotolerant species identified are *Kocuria rhizophila* (found in high relative abundance in sample OM49), and *Salinicoccus qingdaonensis* isolated in the Holy Rock sample RC_wrs_left. These findings are in accordance with the results of previous studies, where most of the investigated building materials presented high content of total soluble salts and many of them high content of NaCl (Apostolopoulou et al., 2018; Moropoulou et al., 2016).

Furthermore, the isolation of the carbonatogenic species of *Acinetobacter johnsonii* in all the investigated samples, and *Pantoea agglomerans* in the samples of the gypsum based mortar Ten_m, the marble OM13 and the lime based mortar SecN3_m, could be proved an important feature; because nowadays there is an increasing interest in such species, as they could be used for the bioremediation of building materials. It is important to point out that bioconsolidation method was developed in 2008 (Gonzalez-Muñoz et al., 2008), and it was based on the selective activation of carbonatogenic microbiota inhabiting stone by the application of a suitable nutritional solution, inducing that way the in situ formation of new calcium carbonate biocement, which effectively consolidates decayed stones. One of the most significant textural features of the newly-formed cement is that it is a biocomposite material made up of an inorganic component ($CaCO_3$) and another (minor) organic component (mainly exopolymeric substance, EPS) (Jimenez-Lopez et al., 2007). In other words, this new cement is a biominerals, with structural and physical mechanical properties that transcend those of the individual components. Since then, many studies have been successfully applied in lab or in pilot scale on monuments, based on the above process, mostly treating calcareous substrates (e.g. (Jroundi et al., 2017)), while a promising in-lab bioconsolidation study of historical gypsum plasters is also recorded (Jroundi et al., 2014). Thus, hopefully in short-term, this environmentally friendly conservation approach is anticipated to be efficiently applied on actual monuments' scale.

3.2 MACHINE LEARNING & CLUSTER ANALYSIS OF METAGENOMICS – DATA CORRELATION IN RELATION WITH BUILDING MATERIALS DATA, ARCHAEOMETRY DATA AND HISTORICAL DATA

Beyond the abundant species detected in all Holy Aedicule samples, there are individual differences that reflect attributes of discrete biodiversity among them. The detection of these species is shadowed by the most abundant communities, yet it offers additional insights for the presence of idiosyncratic mini-communities of microbial co-existence at this unique monument, for the first time.

To achieve this, microbial communities were further assessed by ignoring the most abundant and therefore common species, as mentioned above. The less abundant and yet idiosyncratic communities were ranked at the genus level, to maintain a significant number of read counts, on a per sample basis. At first, hyper-abundant genera with more than 850 reads irrespective of substrate are excluded: those include *Massilia, Pseudomonas, Escherichia* in this order. Next, all other genera with counts between 25 and 850 were also eliminated: these include *Pseudomonas* (644), *Acinetobacter* (175), *Staphylococcus* (97), *Massilia* (81), *Bacillus* (72), *Comamonas* (56), *Psychrobacter* (41), *Aeromonas* (35), *Streptococcus* (31), *Marinobacter* (29), *Hydrogenophaga* (27) and *Enterobacter* (26).

Finally, a simple automated learning method using weighted counts of reads per substrate, reveals the following mini-communities according to the samples, rank ordered as follows: (i) RC_wrs_left and SecN3_wrs: *Chroococcidiopsis, Alkanindiges, Deinococcus, Salinicoccus,* and *Hymenobacter,* (ii) SecN5_mos and OM49: *Chroococcidiopsis*, *Loriellopsis*, (iii) SecN3_m and Ten_m: only *Cutibacterium*, (iv) Arc_m2, OM13 and SecN5_wrs: *Chroococcidiopsis, Loriellopsis, Shigella, Cutibacterium,* and *Ralstonia*. RC_m5 did not exhibit any unique, low-abundance communities, according to the above criteria.

Following the description above about the less abundant communities detected in the Holy Aedicule samples, and the obtained sample associations, we can infer some interesting considerations: First of all, the connotation between RC_wrs_left and SecN3_wrs can be ascribed to their common origin as samples of the Holy Rock; and thus being parts of the original cave, which was used for the Tomb of Christ hewing.

Furthermore, the relation of samples OM49 (marble fragment), and SecN5_mos (mortar sample), exclusively by the photosynthetic genera of *Chroococcidiopsis* and *Loriellopsis*, could be evidence that in some period of the past these materials were not embedded in the Holy Tomb and in the masonry respectively, as they were found; but they were part of Aedicula areas visible to the pilgrims and reached by the sunlight. This result could further support the existing archaeometric evidence briefly described in 2.1 about these two samples (Moropoulou et al., 2018b; Moropoulou et al., 2019). In particular, as regards OM49 marble fragment that it is the decorative edge of the lower fragmented Constantinean plate that was accessed and worshiped by the pilgrims for many centuries; while as far as it concerns the SecN5_mos (a setting bed mortar of a mosaic), that it is part of the alleged mosaic decoration in the Holy Tomb Chamber.

The association of the mortar sample Arc_m2, the marble sample OM13, and the Holy Rock sample SecN5_wrs, through the combination of the low abundance genera *Chroococcidiopsis, Loriellopsis, Shigella, Cutibacterium,* and *Ralstonia,* could reflect the proximity of the sampling locations, of Arc_m2 and SecN5_wrs (Figure 5), as well as the archaeometric data that date Arc_m2 to Constantinean era and interrelate sample OM13 with the same construction period. In particular, the bedding mortar that Arc_m2 was collected from, is above the Holy burial bed rock, the northwest corner of which, is the site of the sample SecN5_wrs. In addition, the Proconnesos marble slab that OM13 is collected from, could have been placed either during the Boniface of Ragusa Restoration, or the Constantinean era; as it is indicated by the OSL results of two mortar samples located in the area of the window permitting the observation of the Holy Rock (Figure 6), (Moropoulou et al., 2018b; Moropoulou et al., 2019). Therefore, if the OM13 marble slab was placed in the Constantinean era, the association of samples Arc_m2 and OM13 regarding the presence of the particular low abundance communities can be justified.

In addition, multivariate, k mean clustering data analysis was performed based on the kind and the abundance of the species identified in each sample. Thus, a heatmap of 16S rDNA amplicons is obtained, where the colour intensity in each panel reflects relative abundances and is used for the correlation analysis (Figure 11). In particular, blue color corresponds to low correlation, white color to medium and red color to high. Cluster analysis includes all the detected species in each sample, excluding however the species that are present only in one sample and with only one read; since no correlation could have been found in any of these cases.

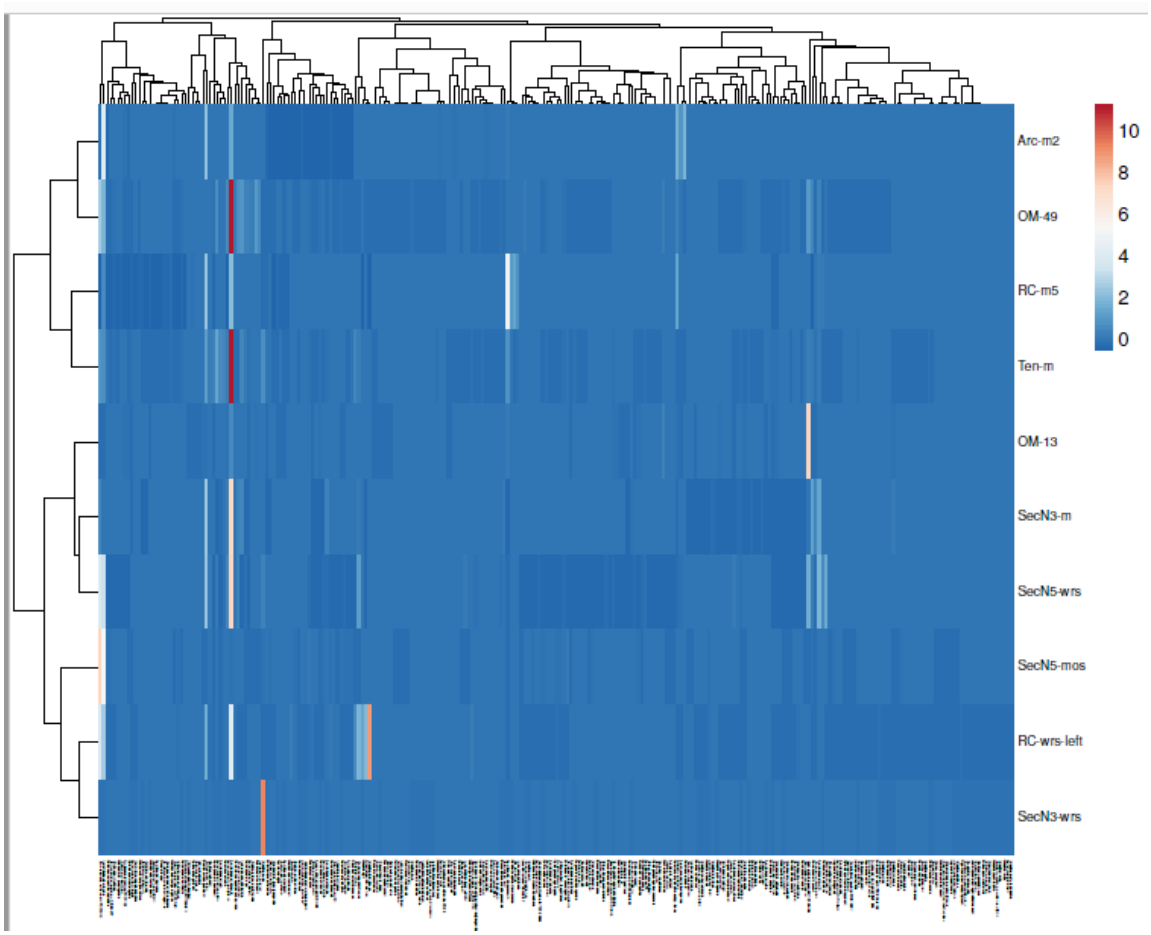

Figure 11. Cluster analysis of all the detected species in each sample. The colour intensity in each panel reflects relative abundances and is used for the correlation analysis (blue: low, white: medium, red: high).

Clustering results showed four different groups of correlated samples in relation to the kind and the abundance of the species identified, which are the following: (a) (RC_wrs_left - Sec_N3_wrs) - SecN5mos; (b) (SecN3_m - SecN5_wrs) - OM13; (c) RC_m5 - Ten_m; and (d) Arc_m2 - OM49.

In the concept that common microbial communities with respective abundance, indicate a relation among samples in regards of microbiota environment, and considering in parallel building materials, archaeometry and historical data, clustering results can be attributed to: (a) Common and/or adjacent location in the building; (b) Production and placement in the building during the same construction period; (c) Common composition/physico-chemical characteristics and production technology.

The first clustering can be ascribed to the fact that RC_wrs_left and SecN3_wrs are both samples of the same building material that is the Holy Rock, collected though from different sampling sites. RC_wrs_left was collected from the Holy Rock embedded in the South masonry of the Holy Tomb Chamber, whereas Sec_N3_wrs was collected from the Holy Rock embedded in the North masonry of the Holy Tomb Chamber (Figures 2, 6, & 7). Both Holy Rock samples are clustered with the gypsum based mortar SecN5_mos, which is dated to the Renaissance era, in 1560 ± 70 CE, at the Restoration of Bonifacio of Ragusa, and was found inside the masonry of Panel N5 at the northwest corner of the Holy Tomb (Figures 2, 4, 5). However, as demonstrated in a previous work (Moropoulou et al., 2018b) and shortly described in 2.1, SecN5_mos is part of the setting bed mortar of a mosaic, and historical testimonies indicate that the Holy Tomb Chamber was adorned by mosaics for some time in the past (Patrich, 2002). Thus, if it is considered that the mosaic actually existed, its original position could be related with the Holy Rock areas of samples RC_wrs_left and/or SecN3_wrs.

The second clustering concerns the lime based mortar sample SecN3_m, the Holy Rock sample of SecN5_wrs and the marble sample OM13. All samples are from different location sites. In particular, the mortar sample was collected from the inner masonry of Panel N3, at the North facade of the Holy Aedicule (Figures 2 & 7), while the Holy Rock sample is part of the northwest corner of the Holy Tomb (Figures 2, 4 & 5). The sample OM13 was collected from a marble facing of the South wall of the Holy Tomb Chamber, opposite to the Holy Tomb, at the area where the observation window of the Holy Rock was installed (Figures 2 & 6). In addition, archaeometric data showed that Sec_N3_m is dated to the Reconstruction of Kalfas Komnenos in 1815 ± 32 CE, whereas OM13 is a Proconnesos marble of variety type 1, and it could have been placed during the Boniface of Ragusa Restoration, without underestimating the possibility that the positioning could have taken place in the Constantinean era (Moropoulou et al., 2018b; Moropoulou et al., 2019). Therefore, their clustering can be attributed to the common chemical composition that the lime based mortar (SecN3_m), the limestone of the Holy Rock (SecN5_wrs) and the Proconnesos marble (OM13) present.

The third clustering is about the gypsum based mortar samples RC_m5 and Ten_m, which were collected from different areas of the monument. The sample RC_m5 is a repair mortar of the large Holy Rock crack located in the South wall of the Holy Tomb Chamber, at the area of the observation window of the Holy Rock (Figures 2 & 6). The sample Ten_m was collected from the North masonry of the low entrance of the Holy Tomb chamber (Figures 2 & 8). As it is briefly presented in 2.1, OSL studies showed that both samples were applied during different construction periods in the monument (Moropoulou et al., 2018b). RC_m5 is dated to the Boniface of Ragusa Restoration in Renaissance (1570 CE), whereas Ten_m is dated most probably to the Byzantine era (1040 ± 150 CE), even though it could belong to the Crusaders era. Thus, the clustering correlation of these two samples is ascribed to their common composition and production technology, since they are both gypsum based mortars presenting gypsum based binder and use of gypsum aggregates except for the calcite ones.

The fourth clustering groups the mortar sample Arc_m2 and the marble fragment OM49, which both were collected from the interior of the Holy Tomb; thus this cluster can be attributed to the common location of the samples (Figures 2, 3 & 5). Considering though the materials data and the archaeometry results, the interrelation of these two samples is further increased, encompassing the criterion of common construction period as well. As described in 2.1, the gypsum based mortar of Arc_m2, was collected from the bedding mortar layer placed between a fragmented grey marble plate, found inside the Tomb, and the Holy burial bed rock. The mortar is dated to the Constantinean era (345 ± 230 CE), and therefore it is deduced that the lower fragmented grey marble plate is also of the Constantinean era (Moropoulou et al., 2018b). Furthermore, this lower grey marble plate is a Proconnesos marble of variety type 1. OM49 is a fragment of Proconnesos marble also of variety type 1, where isotopic results and its thickness justify the assumption that it is part of the fragmented grey marble plate of the Constantinean era (Moropoulou et al., 2019). Consequently, Arc_m2 and OM49 clustering further supports the archaeometry results, where it is pointed out that OM49 could be the decorative edge of the fragmented Constantinean marble plate, indicating that these two materials were positioned at the Holy Tomb during the same construction period, that is the Constantinean era.

4. CONCLUSIONS

Holy Aedicule is a complex structure with almost two millennia turbulent lifetime of destructions and reconstructions. Being an indoor monument is not exposed to direct sunlight, while the temperature and relative humidity variations are evidently lower comparing to outdoor structures. However, the high number of everyday visitors and the intense rising damp from the underground derange this seemingly stable environmental system, increasing thermo-hygric loads. Thus, the development of microbial biodiversity is a multi-factored feature, while its determination is of high importance in terms of the monument's sustainability.

In this work, the detection of the microbiota in marble, mortar and Holy rock samples of the Holy Aedicule was accomplished for the first time, using the approaches of metagenomics and bioinformatics. Successful DNA sampling occurred by non-invasive way, which is an asset for cultural heritage applications. Taxonomic distribution showed that in all samples bacterial sequences represented the 94.16% of the total sequences. Many species of the genus *Pseudomonas* are dominant in all the samples under investigation and particularly the species *Pseudomonas aeruginosa*. Other species such as *Acinetobacter johnsonii, Azotobacter chroococcum, Chroococcidiopsis thermalis PCC 7203, Cutibacterium acnes, Loriellopsis cavernicola, Massilia atriviolacea, Massilia aurea, Staphylococcus saccharolyticus,* and *Zhihengliuella somnathii* are abundant as well.

The isolation of the halotolerant actinobacterium *Zhihengliuella somnathii* in all the samples under investigation, demonstrated the effect of the building materials micro-environment on the microbes development; since previous studies have established that NaCl was evident in most of the building materials of the Holy Aedicule as a result of the intense rising damp. Furthermore, the detection of *Acinetobacter johnsonii* in all the investigated samples, a species with the capacity of inducing $CaCO_3$ precipitation, is a promising finding regarding future applications of materials bioremediation.

The discrete biodiversity among the examined samples was revealed by the application of a machine learning method and the characteristic low abundance communities were ranked at the genus level, to shed light on any unique microbial co-existence. Cluster analysis, based on the kind and the abundance of all the species identified in each sample, resulted in correlation among samples. Both the above mentioned bioinformatics approaches applied, offered additional insights featuring samples interrelation according to sampling location, construction period and/or composition-production technology; thus incorporating materials data, archaeometry data, as well as the historical evidence into the interpretation of the ranked or clustered microbiota communities.

Overall, it is concluded that the elaboration analyses of the metagenomics data through the application of bioinformatics such as machine learning and clustering, as well as the attempt of interpreting these kinds of data in relation to the building materials, archaeometric and historical ones, is an innovative approach that opens a new debate on the potentialities of microbiota characterization in built cultural heritage.

Author Contributions: Conceptualization, A.S. and A.M.; Methodology, E.T.D.; Software, Formal analysis, C.K. and A.C.; Investigation, Data curation, D.V., A.A., V.R., and M.K.; Resources, V.R.; Visualization, C.K., A.A., V.R. and E.T.D.; Writing—original draft preparation, C. K., Z.H., A.C., and T.B.; Writing - review and editing, E.T.D.; Supervision of the experimental DNA extraction, Z.H.; Supervision, C.A.O., A.S. and A.M.; Project administration, A.M. All authors have read and agreed to the published version of the manuscript.

Funding: This research received no external funding. It is a pro bono post-program research, following the rehabilitation of the Holy Aedicule.

ACKNOWLEDGEMENTS

The study and the rehabilitation project of the Holy Aedicule became possible and were executed under the governance of His Beatitude Patriarch of Jerusalem, Theophilos III. The Common Agreement of the Status Quo Christian Communities provided the statutory framework for the execution of the project; His Paternity the Custos of the Holy Land, Archbishop Pierbattista Pizzaballa (until May 2016 – now the Apostolic Administrator of the Latin Patriarchate of Jerusalem), Fr. Francesco Patton (from June 2016), and His Beatitude the Armenian Patriarch of Jerusalem, Nourhan Manougian, authorized His Beatitude the Patriarch of Jerusalem, Theophilos III, and NTUA to perform the project. Contributions from all over the world secured the project's funding. Worth noting Mica Ertegun's and Jack Shear's donations through WMF, Aegean Airlines et al. The interdisciplinary NTUA team for the Protection of Monuments, Em. Korres, A. Georgopoulos, A. Moropoulou, C. Spyrakos, Ch. Mouzakis, were responsible for the rehabilitation project and A. Moropoulou, as Chief Scientific Supervisor, according to the common agreement of the three Christian Communities of the Holy Sepulchre signed on March 22 2016, was responsible for its scientific

supervision. We also acknowledge the major contribution of the DNA Sequence S.R.L. in the metagenomics analysis presented in this work.

Conflicts of Interest: The authors declare no conflict of interest. The funders had no role in the design of the study; in the collection, analyses, or interpretation of data; in the writing of the manuscript, or in the decision to publish the results.

REFERENCES

Adamiak, J., Otlewska, A., Tafer, H., Lopandic, K., Gutarowska, B., Sterflinger, K., & Piñar, G. (2018). First evaluation of the microbiome of built cultural heritage by using the Ion Torrent next generation sequencing platform. *International Biodeterioration and Biodegradation*, *131*. https://doi.org/10.1016/j.ibiod.2017.01.040

Alexakis, E., Delegou, E. T., Lampropoulos, K. C., Apostolopoulou, M., Ntoutsi, I., & Moropoulou, A. (2018). NDT as a monitoring tool of the works progress and the assessment of materials and rehabilitation interventions at the Holy Aedicule of the Holy Sepulchre. *Construction and Building Materials*, *189*. https://doi.org/10.1016/j.conbuildmat.2018.09.007

Apostolopoulou, M., Delegou, E. T., Alexakis, E., Kalofonou, M., Lampropoulos, K. C., Aggelakopoulou, E., Bakolas, A., & Moropoulou, A. (2018). Study of the historical mortars of the Holy Aedicule as a basis for the design, application and assessment of repair mortars: A multispectral approach applied on the Holy Aedicule. *Construction and Building Materials*, *181*. https://doi.org/10.1016/j.conbuildmat.2018.06.016

Banerjee, S., & Joshi, S. (2014). Ultrastructural analysis of calcite crystal patterns formed bybiofilm bacteria associated with cave speleothems. *Journal of Microscopy and Ultrastructure*, *2*(4). https://doi.org/10.1016/j.jmau.2014.06.001

Bauer, M. A., Kainz, K., Carmona-Gutierrez, D., & Madeo, F. (2018). Microbial wars: Competition in ecological niches and within the microbiome. In *Microbial Cell* (Vol. 5, Issue 5). https://doi.org/10.15698/mic2018.05.628

Beneficial Microbes in Agro-Ecology. (2020). In *Beneficial Microbes in Agro-Ecology*. https://doi.org/10.1016/c2020-0-00594-3

Cameron, A., & Hall, S. G. (1981). Eusebius, Life of Constantine. In *Journal of Chemical Information and Modeling* (Vol. 53, Issue 9).

Coyte, K. Z., & Rakoff-Nahoum, S. (2019). Understanding Competition and Cooperation within the Mammalian Gut Microbiome. In *Current Biology* (Vol. 29, Issue 11). https://doi.org/10.1016/j.cub.2019.04.017

Crispim, C. A., & Gaylarde, C. C. (2005). Cyanobacteria and biodeterioration of cultural heritage: A review. In *Microbial Ecology* (Vol. 49, Issue 1). https://doi.org/10.1007/s00248-003-1052-5

Daskalakis, M. I., Magoulas, A., Kotoulas, G., Catsikis, I., Bakolas, A., Karageorgis, A. P., Mavridou, A., Doulia, D., & Rigas, F. (2013). Pseudomonas, Pantoea and Cupriavidus isolates induce calcium carbonate precipitation for biorestoration of ornamental stone. *Journal of Applied Microbiology*, *115*(2). https://doi.org/10.1111/jam.12234

David, L. A., Maurice, C. F., Carmody, R. N., Gootenberg, D. B., Button, J. E., Wolfe, B. E., Ling, A. V., Devlin, A. S., Varma, Y., Fischbach, M. A., Biddinger, S. B., Dutton, R. J., & Turnbaugh, P. J. (2014). Diet rapidly and reproducibly alters the human gut microbiome. *Nature*, *505*(7484). https://doi.org/10.1038/nature12820

de Leo, F., Iero, A., Zammit, G., & Urzì, C. E. (2012). Chemoorganotrophic bacteria isolated from biodeteriorated surfaces in cave and catacombs. *International Journal of Speleology*, *41*(2). https://doi.org/10.5038/1827-806X.41.2.1

De Los Ríos, A., Grube, M., Sancho, L. G., & Ascaso, C. (2007). Ultrastructural and genetic characteristics of endolithic cyanobacterial biofilms colonizing Antarctic granite rocks. *FEMS Microbiology Ecology*, *59*(2). https://doi.org/10.1111/j.1574-6941.2006.00256.x

Delgado Rodrigues, J., & Ferreira Pinto, A. P. (2019). Stone consolidation by biomineralisation. Contribution for a new conceptual and practical approach to consolidate soft decayed limestones. *Journal of Cultural Heritage*, *39*. https://doi.org/10.1016/j.culher.2019.04.022

DI Tommaso, P., Chatzou, M., Floden, E. W., Barja, P. P., Palumbo, E., & Notredame, C. (2017). Nextflow enables reproducible computational workflows. In *Nature Biotechnology* (Vol. 35, Issue 4). https://doi.org/10.1038/nbt.3820

Dyda, M., Pyzik, A., Wilkojc, E., Kwiatkowska-Kopka, B., & Sklodowska, A. (2019). Bacterial and fungal diversity inside the medieval building constructed with sandstone plates and lime mortar as an example of the microbial colonization of a nutrient-limited extreme environment (Wawel royal castle, Krakow, Poland). *Microorganisms*, *7*(10). https://doi.org/10.3390/microorganisms7100416

Evison, M. P. (2014). Genetics, archaeology and culture. *Mediterranean Archaeology and Archaeometry*, *14*(1). https://doi.org/10.5281/zenodo.14334

Freeman, F. (1947). *Church of the Holy Sepulchre Jerusalem : report*. Freeman Fox & Partners consulting engineers.

Funkhouser, L. J., & Bordenstein, S. R. (2013). Mom Knows Best: The Universality of Maternal Microbial Transmission. *PLoS Biology*, *11*(8). https://doi.org/10.1371/journal.pbio.1001631

Gallego, V., Sánchez-Porro, C., García, M. T., & Ventosa, A. (2006). Massilia aurea sp. nov., isolated from drinking water.

International Journal of Systematic and Evolutionary Microbiology, *56*(10), 2449–2453. https://doi.org/10.1099/ijs.0.64389-0

Georgopoulos, A., Lambrou, E., Pantazis, G., Agrafiotis, P., Papadaki, A., Kotoula, L., Lampropoulos, K., Delegou, E., Apostolopoulou, M., Alexakis, M., & Moropoulou, A. (2017). Merging geometric documentation with materials characterization and analysis of the history of the holy aedicule in the church of the holy sepulchre in Jerusalem. *International Archives of the Photogrammetry, Remote Sensing and Spatial Information Sciences - ISPRS Archives*, *42*(5W1). https://doi.org/10.5194/isprs-Archives-XLII-5-W1-487-2017

Gu, J. D. (2007). Microbial colonization of polymeric materials for space applications and mechanisms of biodeterioration: A review. *International Biodeterioration and Biodegradation*, *59*(3 SPEC. ISS.), 170–179. https://doi.org/10.1016/j.ibiod.2006.08.010

Gumaelius, L., Magnusson, G., Pettersson, B., & Dalhammar, G. (2001). Comamonas denitrificans sp. nov., an efficient denitrifying bacterium isolated from activated sludge. *International Journal of Systematic and Evolutionary Microbiology*, *51*(3). https://doi.org/10.1099/00207713-51-3-999

Hammer, T. J., Sanders, J. G., & Fierer, N. (2019). Not all animals need a microbiome. In *FEMS Microbiology Letters* (Vol. 366, Issue 10). https://doi.org/10.1093/femsle/fnz117

Hsu, Y. H., Lai, W. A., Lin, S. Y., Hameed, A., Shahina, M., Shen, F. T., Zhu, Z. L., Young, L. Sen, & Young, C. C. (2013). Chiayiivirga flava gen. nov., sp. nov., a novel bacterium of the family Xanthomonadaceae isolated from an agricultural soil, and emended description of the genus Dokdonella. *International Journal of Systematic and Evolutionary Microbiology*, *63*(PART9). https://doi.org/10.1099/ijs.0.048579-0

Hyun, D. W., Whon, T. W., Cho, Y. J., Chun, J., Kim, M. S., Jung, M. J., Shin, N. R., Kim, J. Y., Kim, P. S., Yun, J. H., Lee, J., Oh, S. J., & Bae, J. W. (2013). Genome sequence of the moderately halophilic bacterium Salinicoccus carnicancri type strain CrmT (= DSM 23852T). *Standards in Genomic Sciences*, *8*(2). https://doi.org/10.4056/sigs.3967649

Jha, B., Kumar Singh, V., Weiss, A., Hartmann, A., Schmid, M., Singh, V. K., Weiss, A., Hartmann, A., & Schmid, M. (2015). Zhihengliuella somnathii sp. nov., a halotolerant actinobacterium from the rhizosphere of a halophyte Salicornia brachiata. *International Journal of Systematic and Evolutionary Microbiology*, *65*(9), 3137–3142. https://doi.org/10.1099/ijsem.0.000391

Jimenez-Lopez, C., Rodriguez-Navarro, C., Piñar, G., Carrillo-Rosúa, F. J., Rodriguez-Gallego, M., & Gonzalez-Muñoz, M. T. (2007). Consolidation of degraded ornamental porous limestone stone by calcium carbonate precipitation induced by the microbiota inhabiting the stone. *Chemosphere*, *68*(10). https://doi.org/10.1016/j.chemosphere.2007.02.044

Jroundi, F., Gonzalez-Muñoz, M. T., Garcia-Bueno, A., & Rodriguez-Navarro, C. (2014). Consolidation of archaeological gypsum plaster by bacterial biomineralization of calcium carbonate. *Acta Biomaterialia*, *10*(9). https://doi.org/10.1016/j.actbio.2014.03.007

Jroundi, F., Schiro, M., Ruiz-Agudo, E., Elert, K., Martín-Sánchez, I., González-Muñoz, M. T., & Rodriguez-Navarro, C. (2017). Protection and consolidation of stone heritage by self-inoculation with indigenous carbonatogenic bacterial communities. *Nature Communications*, *8*(1). https://doi.org/10.1038/s41467-017-00372-3

Kiledal, E. A., Keffer, J. L., & Maresca, J. A. (2021). Bacterial Communities in Concrete Reflect Its Composite Nature and Change with Weathering. *MSystems*, *6*(3). https://doi.org/10.1128/msystems.01153-20

Kim, D., Song, L., Breitwieser, F. P., & Salzberg, S. L. (2016). Centrifuge: Rapid and sensitive classification of metagenomic sequences. *Genome Research*, *26*(12). https://doi.org/10.1101/gr.210641.116

Kloos, W. E., & Schleifer, K. H. (1975). Isolation and characterization of Staphylococci from human skin. II. Descriptions of four new species: Staphylococcus warneri, Staphylococcus capitis, Staphylococcus hominis, and Staphylococcus simulans. *International Journal of Systematic Bacteriology*, *25*(1). https://doi.org/10.1099/00207713-25-1-62

Kunin, V., Copeland, A., Lapidus, A., Mavromatis, K., & Hugenholtz, P. (2008). A Bioinformatician's Guide to Metagenomics. *Microbiology and Molecular Biology Reviews*, *72*(4), 557–578. https://doi.org/10.1128/mmbr.00009-08

Kwiatkowski, D., & Löfvendahl, R. (2005). Proceedings of the 10th International Congress on Deterioration and Conservation of Stone: Stockholm, June 27-July 2, 2004. In *Stone 2004 The 10th International Congress on Detorioration and Conservation of Stone Stockholm 27 June2 July 2004*.

Lamprinou, V., Hernández-Mariné, M., Canals, T., Kormas, K., Economou-Amilli, A., & Pantazidou, A. (2011). Morphology and molecular evaluation of iphinoe spelaeobios gen. nov., sp. nov. and Loriellopsis cavernicola gen. nov., sp. nov., two stigonematalean cyanobacteria from Greek and Spanish caves. *International Journal of Systematic and Evolutionary Microbiology*, *61*(12). https://doi.org/10.1099/ijs.0.029223-0

Lampropoulos, K. C., Apostolopoulou, M., Tsilimantou, E., & Moropoulou, A. (2022). *The Grouting Process as an Innovative Tool for the Assessment of the State of Preservation and Internal Features of the Holy Aedicule of the Holy Sepulchre*. 61–87.

Lampropoulos, K. C., Moropoulou, A., & Korres, M. (2017). Ground penetrating radar prospection of the construction phases of the Holy Aedicula of the Holy Sepulchre in correlation with architectural analysis. *Construction and Building Materials*, *155*. https://doi.org/10.1016/j.conbuildmat.2017.08.044

Liritzis, I., Hilioti, Z., Karapiperis, C., Valasiadis, D., Alexandridou, A., & Rihani, V. (2021). Whole Genome Sequencing Approach Revealed Species in Mycenaean Period Associated Residual Plant Biomass: First Results. *Mediterranean Archaeology and Archaeometry*, *21*(3), 229–247. https://doi.org/10.5281/zenodo.5598249

Luz Calle, M. (2019). Statistical analysis of metagenomics data. In *Genomics and Informatics* (Vol. 17, Issue 1).

https://doi.org/10.5808/GI.2019.17.1.e6

Mazzoli, R., Giuffrida, M. G., & Pessione, E. (2018). Back to the past: "find the guilty bug—microorganisms involved in the biodeterioration of archeological and historical artifacts." In *Applied Microbiology and Biotechnology* (Vol. 102, Issue 15). https://doi.org/10.1007/s00253-018-9113-3

McNamara, C. J., Perry IV, T. D., Bearce, K. A., Hernandez-Duque, G., & Mitchell, R. (2006). Epilithic and endolithic bacterial communities in limestone from a Maya archaeological site. *Microbial Ecology*, *51*(1). https://doi.org/10.1007/s00248-005-0200-5

Meško, M. (2016). How to reverse the decline of an empire? two byzantine case studies: Herakleios and alexios komnenos. In *Graeco-Latina Brunensia* (Vol. 21, Issue 1). https://doi.org/10.5817/GLB2016-1-6

Metsalu, T., & Vilo, J. (2015). ClustVis: A web tool for visualizing clustering of multivariate data using Principal Component Analysis and heatmap. *Nucleic Acids Research*, *43*(W1). https://doi.org/10.1093/nar/gkv468

Meunier, R., & Bayır, S. (2021). Metagenomics approaches in microbial ecology and research for sustainable agriculture. *TATuP - Zeitschrift Für Technikfolgenabschätzung in Theorie Und Praxis*, *30*(2). https://doi.org/10.14512/tatup.30.2.24

Mihajlovski, A., Gabarre, A., Seyer, D., Bousta, F., & Di Martino, P. (2017). Bacterial diversity on rock surface of the ruined part of a French historic monument: The Chaalis abbey. *International Biodeterioration and Biodegradation*, *120*. https://doi.org/10.1016/j.ibiod.2017.02.019

Mitropoulos, T. (2009). The Church of Holy Sepulchre—The Work of Kalfas Komnenos. *European Centre of Byzantine and Post-Byzantine Monuments: Thessaloniki, Greece*.

Moropoulou, A., Delegou, E. T., Apostolopoulou, M., Kolaiti, A., Papatrechas, C., Economou, G., & Mavrogonatos, C. (2019). The white marbles of the Tomb of Christ in Jerusalem: Characterization and provenance. *Sustainability (Switzerland)*, *11*(9). https://doi.org/10.3390/su11092495

Moropoulou, A., Georgopoulos, A., Korres, M., Bakolas, A., Labropoulos, K., Agrafiotis, P., Delegou, E. T., Moundoulas, P., Apostolopoulou, M., Lambrou, E., Pantazis, G., Kotoula, L., Papadaki, A., & Alexakis, E. (2017). Five-Dimensional (5D) Modelling of the Holy Aedicule of the Church of the Holy Sepulchre Through an Innovative and Interdisciplinary Approach. In *Mixed Reality and Gamification for Cultural Heritage*. https://doi.org/10.1007/978-3-319-49607-8_9

Moropoulou, A., Korres, E., Georgopoulos, A., & Spyrakos, C. (2016). *Materials and Conservation, Reinforcement and Rehabilitation Interventions in the Holy Edicule of the Holy Sepulchre*.

Moropoulou, A., Korres, M., Georgopoulos, A., Spyrakos, C., Mouzakis, C., Lampropoulos, K. C., & Apostolopoulou, M. (2018). *The Project of the Rehabilitation of Holy Sepulchre's Holy Aedicule as a Pilot Multispectral, Multidimensional, Novel Approach Through Transdisciplinarity and Cooperation in the Protection of Monuments*. Springer International Publishing.

Moropoulou, A., Zacharias, N., Delegou, E. T., Apostolopoulou, M., Palamara, E., & Kolaiti, A. (2018). OSL mortar dating to elucidate the construction history of the Tomb Chamber of the Holy Aedicule of the Holy Sepulchre in Jerusalem. *Journal of Archaeological Science: Reports*, *19*. https://doi.org/10.1016/j.jasrep.2018.02.024

Nir, I., Barak, H., Kramarsky-Winter, E., Kushmaro, A., & de los Ríos, A. (2021). Microscopic and biomolecular complementary approaches to characterize bioweathering processes at petroglyph sites from the Negev Desert, Israel. *Environmental Microbiology*. https://doi.org/10.1111/1462-2920.15635

Patrich, J. (2002). The edicule in the Church of the Holy Sepulchre - Martin Biddle, THE TOMB OF CHRIST (Sutton Publishing Ltd., Stroud, Glos. 1999). Pp. xii 172, 103 figs. including colour. *Journal of Roman Archaeology*, *Journal of*, 688–690. https://doi.org/10.1017/S1047759400014641

Piñar, G., Poyntner, C., Tafer, H., & Sterflinger, K. (2019). A time travel story: metagenomic analyses decipher the unknown geographical shift and the storage history of possibly smuggled antique marble statues. *Annals of Microbiology*, *69*(10). https://doi.org/10.1007/s13213-019-1446-3

Ramazzotti, M., & Bacci, G. (2018). 16S rRNA-Based Taxonomy Profiling in the Metagenomics Era. *Metagenomics: Perspectives, Methods, and Applications*, 103–119. https://doi.org/10.1016/B978-0-08-102268-9.00005-7

Sanmartín, P., Bosch-Roig, P., Gulotta, D., Fort, R., Bosch, I., & Cappitelli, F. (2021). Klebsiella aerogenes and Comamonas testosteroni as bioremoval agents on graffiti-coated concrete and granite: Impact assessment through surface analysis. *International Biodeterioration and Biodegradation*, *161*. https://doi.org/10.1016/j.ibiod.2021.105244

Schmeisser, C., Steele, H., & Streit, W. R. (2007). Metagenomics, biotechnology with non-culturable microbes. In *Applied Microbiology and Biotechnology* (Vol. 75, Issue 5). https://doi.org/10.1007/s00253-007-0945-5

Schommer, N. N., & Gallo, R. L. (2013). Structure and function of the human skin microbiome. In *Trends in Microbiology* (Vol. 21, Issue 12). https://doi.org/10.1016/j.tim.2013.10.001

Schröer, L., Boon, N., De Kock, T., & Cnudde, V. (2021). The capabilities of bacteria and archaea to alter natural building stones – A review. In *International Biodeterioration and Biodegradation* (Vol. 165). https://doi.org/10.1016/j.ibiod.2021.105329

Skipper, P. (2018). *"Biodeterioration of limestone: role of bacterial biofilms and possible intervention strategies"*. University of Lincoln.

Smith, H. D., Baqué, M., Duncan, A. G., Lloyd, C. R., McKay, C. P., & Billi, D. (2014). Comparative analysis of cyanobacteria inhabiting rocks with different light transmittance in the Mojave Desert: A Mars terrestrial analogue. *International Journal of Astrobiology*, *13*(3). https://doi.org/10.1017/S1473550414000056

Takarada, H., Sekine, M., Kosugi, H., Matsuo, Y., Fujisawa, T., Omata, S., Kishi, E., Shimizu, A., Tsukatani, N., Tanikawa, S., Fujita, N., & Harayama, S. (2008). Complete genome sequence of the soil actinomycete Kocuria rhizophila. *Journal of Bacteriology*, *190*(12). https://doi.org/10.1128/JB.01853-07

Teasdale, M. D., Fiddyment, S., Vnouček, J., Mattiangeli, V., Speller, C., Binois, A., Carver, M., Dand, C., Newfield, T. P., Webb, C. C., Bradley, D. G., & Collins, M. J. (2017). The york gospels: A 1000-year biological palimpsest. *Royal Society Open Science*, *4*(10). https://doi.org/10.1098/rsos.170988

Vilanova, C., & Porcar, M. (2020). Art-omics: multi-omics meet archaeology and art conservation. *Microbial Biotechnology*, *13*(2), 435–441. https://doi.org/10.1111/1751-7915.13480

Vishnivetskaya, T. A., Kathariou, S., & Tiedje, J. M. (2009). The Exiguobacterium genus: Biodiversity and biogeography. *Extremophiles*, *13*(3). https://doi.org/10.1007/s00792-009-0243-5

Wei, F., Wu, Q., Hu, Y., Huang, G., Nie, Y., & Yan, L. (2019). Conservation metagenomics: a new branch of conservation biology. In *Science China Life Sciences* (Vol. 62, Issue 2). https://doi.org/10.1007/s11427-018-9423-3

Weon, H. Y., Kim, B. Y., Son, J. A., Jang, H. B., Hong, S. K., Go, S. J., & Kwon, S. W. (2008). Massilia aerilata sp. nov., isolated from an air sample. *International Journal of Systematic and Evolutionary Microbiology*, *58*(6), 1422–1425. https://doi.org/10.1099/ijs.0.65419-0

Wynn-Williams, D. D. (2006). Cyanobacteria in Deserts — Life at the Limit? In *The Ecology of Cyanobacteria*. https://doi.org/10.1007/0-306-46855-7_13

Zhang, B., Yang, R., Zhang, G., Zhang, D., Zhang, W., Chen, T., & Liu, G. (2020). Massilia arenae sp. Nov., isolated from sand soil in the qinghai– tibetan plateau. *International Journal of Systematic and Evolutionary Microbiology*, *70*(4), 2435–2439. https://doi.org/10.1099/ijsem.0.004056

Zhou, E., Li, H., Yang, C., Wang, J., Xu, D., Zhang, D., & Gu, T. (2018). Accelerated corrosion of 2304 duplex stainless steel by marine Pseudomonas aeruginosa biofilm. *International Biodeterioration and Biodegradation*, *127*. https://doi.org/10.1016/j.ibiod.2017.11.003

Zul, D., Wanner, G., & Overmann, J. (2008). Massilia brevitalea sp. nov., a novel betaproteobacterium isolated from lysimeter soil. *International Journal of Systematic and Evolutionary Microbiology*, *58*(5), 1245–1251. https://doi.org/10.1099/ijs.0.65473-0